

# **ANNEXURE**

Silica Encapsulated Stabilized  
PdNCLs by TPA: Synthesis,  
Characterization and  
Applications to C-C coupling  
and Hydrogenation



# Designing of Highly Active and Sustainable Encapsulated Stabilized Palladium Nanoclusters as well as Real Exploitation for Catalytic Hydrogenation in Water

Anish Patel and Anjali Patel\*

Polyoxometalates and Catalysis Laboratory, Department of Chemistry, Faculty of Science.

The Maharaja Sayajirao University of Baroda. Vadodara-390002. Gujarat. India.

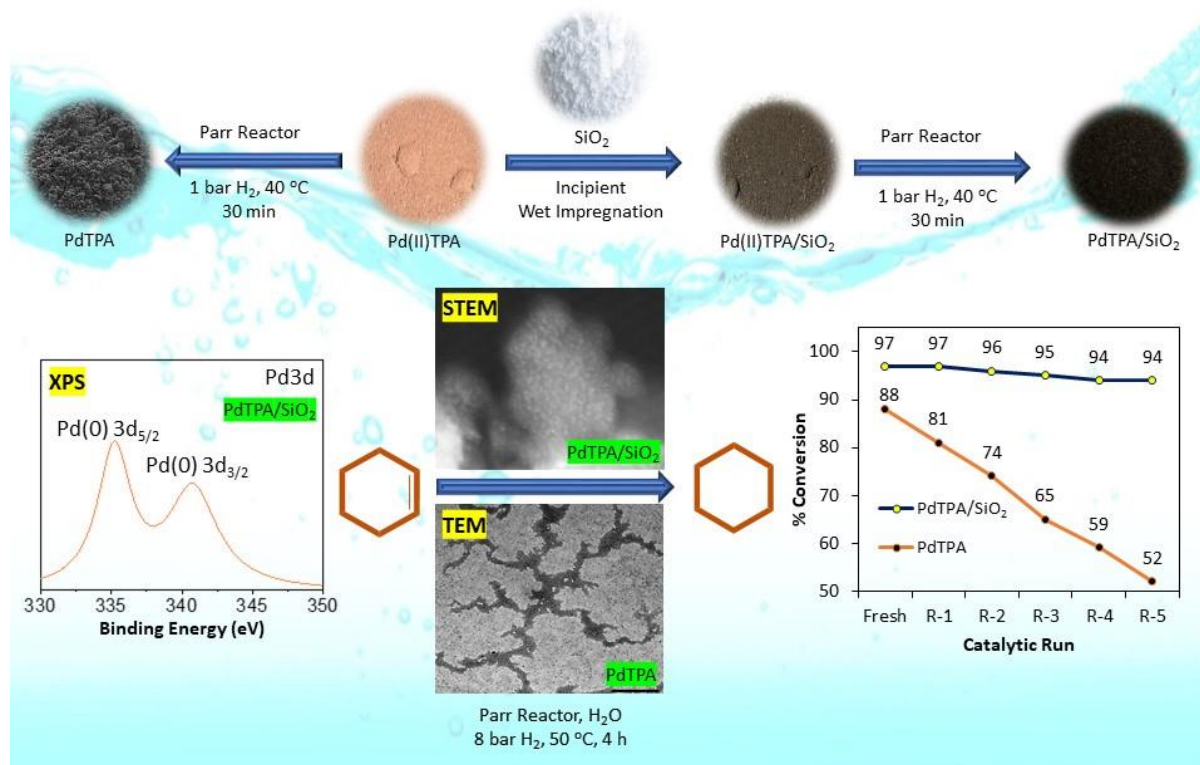
\*E-mail: [anjali.patel-chem@msubaroda.ac.in](mailto:anjali.patel-chem@msubaroda.ac.in)

ORCID: 0000-0002-6871-7564 and 0000-0003-0177-3956\*

## Abstract

Encapsulated nanoclusters based on palladium, 12-tunstophosphoric acid and silica was designed by simple wet impregnation methodology. The catalyst was found to be very efficient towards cyclohexene hydrogenation up to five catalytic runs with substrate/catalyst ratio of 4377/1 at 50 °C as well as for alkene, aldehyde, nitro and halogen compounds.

*Accepted, Catalysis Letters. DOI: 10.1007/s10562-020-03327-4*





The outstanding activity of the synthesized materials based on stabilized PdNCs in both C-C coupling as well as hydrogenation, encouraged us to design other catalysts using different support for the same applications, in order to investigate the effect of support on the reactions.

For the same, we have selected another effective metal oxide support, silica ( $\text{SiO}_2$ ). Mesoporous silica materials are, indeed, ideal acidic supports for PdNCs, since they exhibit high surface area and their inner and outer surfaces have a profusion of pendant silanol groups (generally, from 1 to 3 OH groups per square nanometer) that are optimal loci for encapsulation of more than a quarter periodic table elements as an active catalytic site [1, 2]. Because of their high porosity, feasible potential grafting sites to enhance the activity [3-5], such catalysts facilitate ingress of reactants to, and the egress of products from, the active centres [6].

As in the case of  $\text{ZrO}_2$ , we designed  $\text{SiO}_2$  based nanocatalysts by both methods. However, we could not synthesize the catalysts Pd-TPA/ $\text{SiO}_2$  as well as Pd-LTPA/ $\text{SiO}_2$ , i.e. by ion exchange method. We believe that this may be due to higher acidity of  $\text{SiO}_2$  as compare to that of  $\text{ZrO}_2$  and can be explained on the basis of **Point of Zero Charge (PZC)**.

#### **Point of Zero Charge (PZC)**

The surface of metal oxide is always active and therefore, the oxide surface immediately reacts with water molecules to form hydroxyl groups as shown in figure 1a. The surface hydroxyl groups contain both terminal OH and bridge OH in the equal amounts. Active surface hydroxyl groups dissociate in aqueous solutions and forms electric charges [7-9] as shown in figure 1b. Positive or negative charge due to the dissociation is governed by pH of the surrounding aqueous solution: positive and negative charges are balanced and apparent charge is zero at a certain pH. The pH at which the surface of adsorbent is globally neutral, i.e., contains as much positively charged as negatively charged surface functions called PZC. Metal oxides have unique PZC values. In other

words, surface is acidic when  $\text{pH} < \text{PZC}$  and basic at  $\text{pH} > \text{PZC}$  (Figure 1b) [10]. Active surface hydroxyl groups and electric charges formed by the dissociation of the groups at certain pH play important roles for the bonding with TPA.

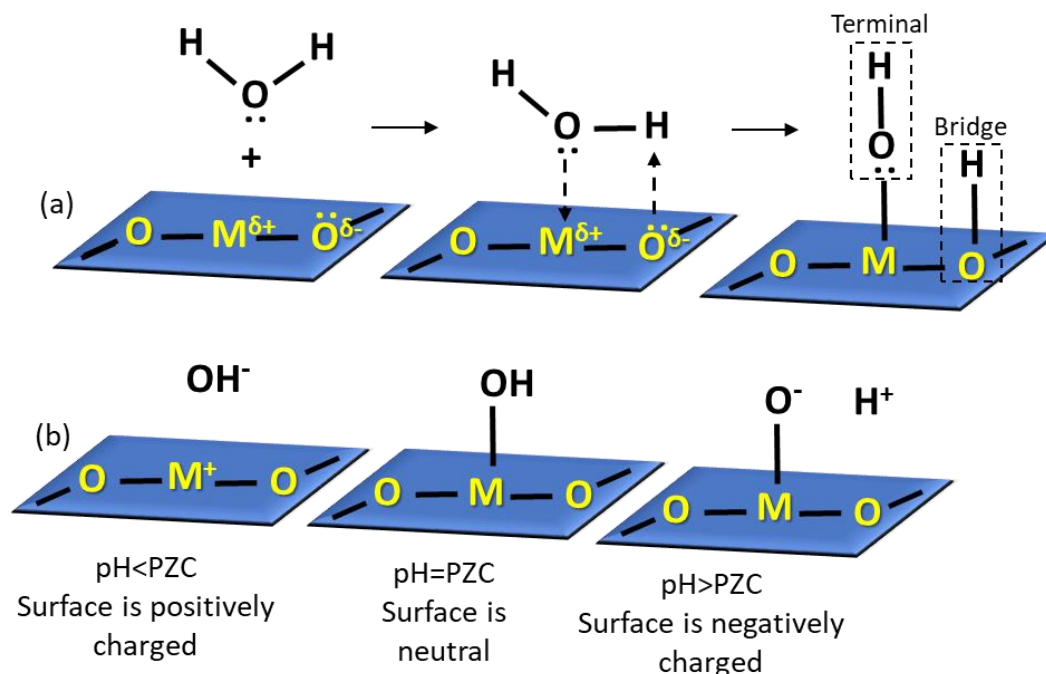


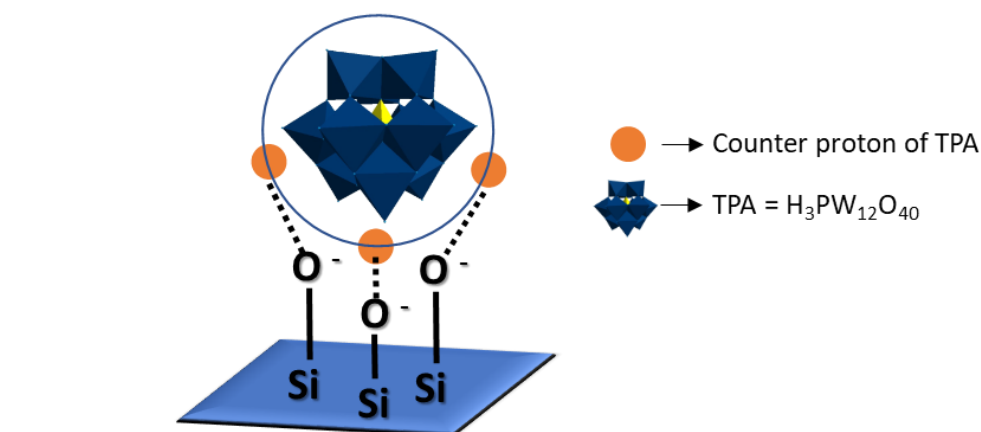
**Figure 1** (a) Formation of surface hydroxyl group over metal oxide support and (b) Effect of pH on surface charge.

In case of  $\text{ZrO}_2$  support, the PZC values is 8 [11], which is higher than pH of 1 % aq. TPA (pH=2.8). As discussed above, when  $\text{pH} < \text{PZC}$ , the surface of  $\text{ZrO}_2$  will be positively charged. The positively charged zirconium of  $\text{ZrO}_2$  will interact with terminal oxygen of TPA and as a result, the counter protons remain available to be exchanged with another metal, in the present case, Pd.

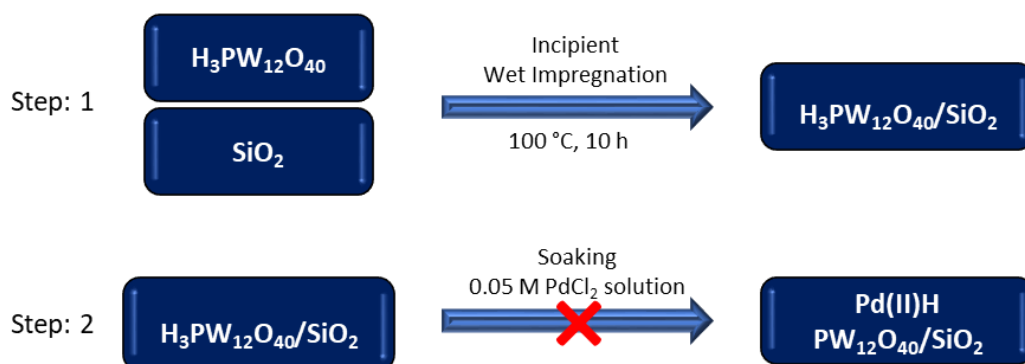
Whereas, PZC value of silica is 2.5 [12], which is smaller than pH of 1 % aq. TPA (pH, 2.8). As a result, the surface of support (here,  $\text{SiO}_2$ ) will be negatively charged [12]. As mentioned earlier (Page No. 53), ion-exchange method involves supporting of TPA onto support followed by exchange of protons. Here, the negatively charged oxygen of  $\text{SiO}_2$  will interact with protons of TPA and as a result, these occupied protons will not be available for exchange with the Pd of

$\text{PdCl}_2$  during soaking. Hence, this method is not feasible for such materials having low PZC values. For better understanding, schematic representation is shown in scheme 1. Salt method is the alternative one for the synthesis of catalysts having such type of supports.

pH of 1 % aq.  $\text{H}_3\text{PW}_{12}\text{O}_{40} = 2.8$   
 PZC of  $\text{SiO}_2 = 2.5$  }  $\text{pH} > \text{PZC} \longrightarrow \text{Surface of } \text{SiO}_2 \text{ is negatively charged}$



#### Ion Exchange method



Because, there is no available free protons to be exchanged

**Scheme 1** Schematic representation of co-relation between pH, PZC and surface charge of  $\text{SiO}_2$ ; effect of interaction between TPA and  $\text{SiO}_2$  on exchange method.

In this chapter, we report the encapsulation of PdTPA into silica ( $\text{PdTPA}/\text{SiO}_2$ ) by impregnation and post reduction method. The catalyst was characterized by EDX, TGA, BET, FT-IR,  $^{31}\text{P}$  MAS NMR, powder XRD, XPS, TEM, HRTEM and BF & DF-STEM. The efficiency of the catalyst was evaluated as a sustainable

heterogeneous catalyst for C-C coupling (SM and Heck) and hydrogenation. Influence of various parameters such as catalyst amount, temperature, pressure, time, base, solvent, solvent ratio was studied for respective reactions to obtain maximum conversion. The catalyst was retrieved by simple centrifugation, regenerated at just 100 °C and reused up to five cycles. The regenerated catalyst was characterized by various characterization techniques to confirm its sustainability. The viability was also examined towards different substrates as well as comparison with the previously reported systems was also surveyed. Mechanistic investigation has been studied via performing reaction using D<sub>2</sub>O as solvent. Effect of support on the reactions was also discussed.



## EXPERIMENTAL

### Materials

All chemicals used were of A. R. grade. 12-tungstophosphoric acid, silica (60-120 mesh), palladium chloride, iodobenzene, phenylboronic acid, styrene, dimethyl formamide, potassium carbonate, cyclohexene, petroleum ether, ethyl acetate and dichloromethane were obtained from Merck and used as received.

### Catalyst Synthesis

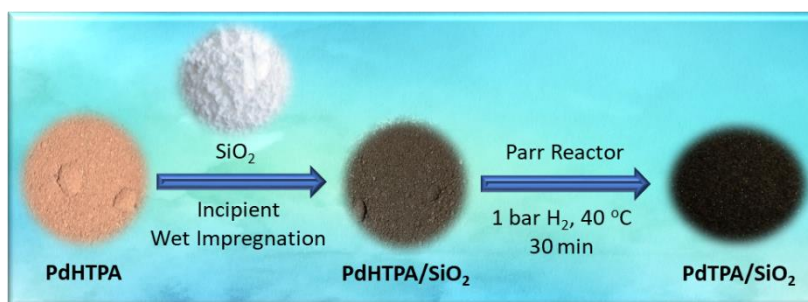
Silica encapsulated stabilized palladium tungstophosphoric acid (PdTPA/SiO<sub>2</sub>) was synthesized by top-down non-covalent deposition in two steps.

*Step-1: Synthesis of 12-tungstophosphoric acid stabilized PdNCLs (PdTPA).*

PdTPA was synthesized as discussed in Part-B\_Chapter-1.

*Step-2: Synthesis of Silica encapsulated PdTPA (PdTPA/SiO<sub>2</sub>)*

A series of materials, containing 10-40 % of Pd(II)TPA encapsulated into SiO<sub>2</sub> was synthesized by incipient wet impregnation method. 1 g of SiO<sub>2</sub> was impregnated with aqueous solution of Pd(II)TPA (0.1/10-0.4/40 g mL<sup>-1</sup> of double distilled water) and dried at 100 °C for 10 h, finally treated under 1 bar H<sub>2</sub> pressure at 40 °C for 30 min using Parr reactor. The obtained materials with 10-40 % loading was designated as 10 % PdTPA/SiO<sub>2</sub>, 20 % PdTPA/SiO<sub>2</sub>, 30 % PdTPA/SiO<sub>2</sub> (Later, PdTPA/SiO<sub>2</sub>) and 40 % PdTPA/SiO<sub>2</sub> respectively. The synthetic scheme of PdTPA/SiO<sub>2</sub> is shown in scheme 2.



**Scheme 2** Synthetic scheme of PdTPA/SiO<sub>2</sub>.

## Catalytic Evaluation

The C-C coupling and hydrogenation reactions were carried out following the same procedure as mentioned in Part-A\_Chapter 1.

The effect of loading on all the three reactions was evaluated by varying % loading of PdTPA (10-40 %) into SiO<sub>2</sub>. The obtained results (Figure 2) show that conversion increases with an increase in % loading from 10 to 30 % PdTPA into SiO<sub>2</sub>. However, further increase in loading from 30 to 40 % results no positive change in conversion, which may be due to the blocking of active sites in the catalysts. Hence, 30% PdTPA/SiO<sub>2</sub> (Later, PdTPA/SiO<sub>2</sub>) catalyst was selected for detailed characterization and catalytic study.

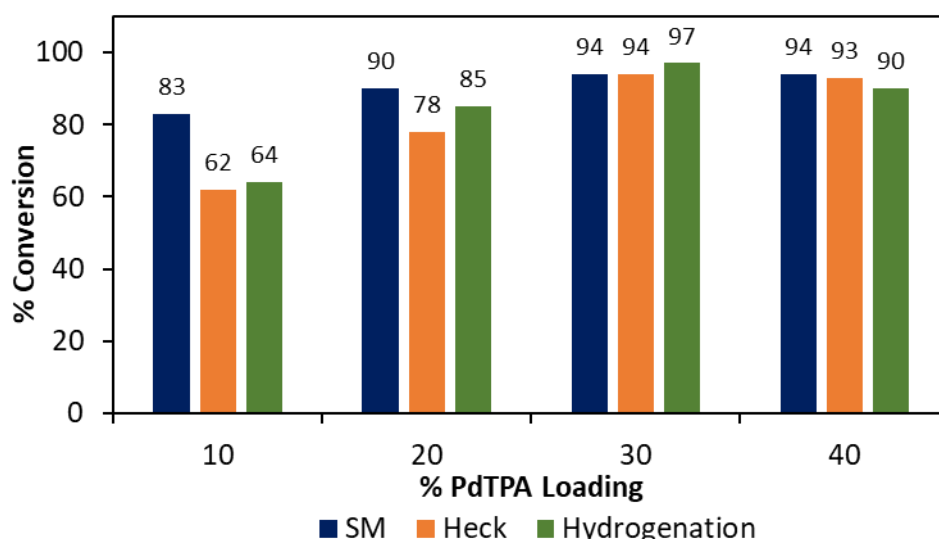


**Figure 2** Effect of PdTPA loading. Reaction condition: *SM coupling*- iodobenzene (1.96 mM), phenylboronic acid (2.94 mM), catalyst (0.0192 mol% Pd), K<sub>2</sub>CO<sub>3</sub> (3.92 mmol), C<sub>2</sub>H<sub>5</sub>OH: H<sub>2</sub>O (3:7 mL), temperature (90 °C), time (30 min); *Heck coupling*- iodobenzene (0.98 mM), styrene (1.47 mM), catalyst (0.115 mol% Pd), K<sub>2</sub>CO<sub>3</sub> (1.96 mmol), DMF: H<sub>2</sub>O (3:2 mL), temperature (100 °C), time (6 h); *Hydrogenation*- cyclohexene (9.87 mmol), catalyst (0.023 mol% Pd), H<sub>2</sub>O (50 mL), temperature (80 °C), H<sub>2</sub> pressure (10 bar), time (4 h).

## RESULTS AND DISCUSSION

### Catalyst Characterization

The gravimetric analysis of Pd (3.52 wt %) and W (74.40 wt %) in PdTPA were in good agreement with the theoretical values (3.60 wt % and 74.59 wt %, respectively) as well as EDX values (3.46 wt % and 74.87 wt %, respectively). For PdTPA/SiO<sub>2</sub>, analytical values of W (17.43 wt %) and Pd (0.80 wt %) were also in good agreement with theoretical values, W (17.21 wt %) and Pd (0.82 wt %). EDX elemental mapping of the catalysts is shown in figure 3.

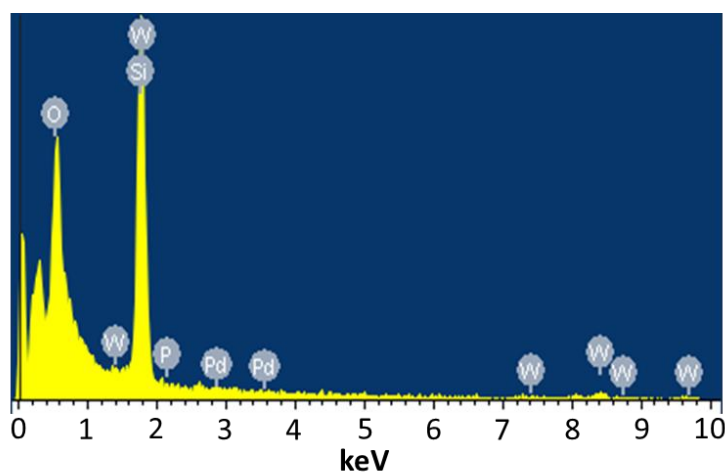


**Figure 3** EDX mapping of PdTPA/SiO<sub>2</sub>.

TGA of PdTPA (Figure 4) shows 0.8 % weight loss, adsorbed water, in the temperature range of 70-120 °C. While, 3.0 % weight loss up to 190 °C, indicating the loss of crystalline water molecules. Whereas, PdTPA/SiO<sub>2</sub> shows an initial weight loss of 2.3 % up to 150 °C, indicating the loss of adsorbed water molecules. Besides this, no significant weight loss was observed up to 500 °C, suggesting higher thermal stability of the catalyst.

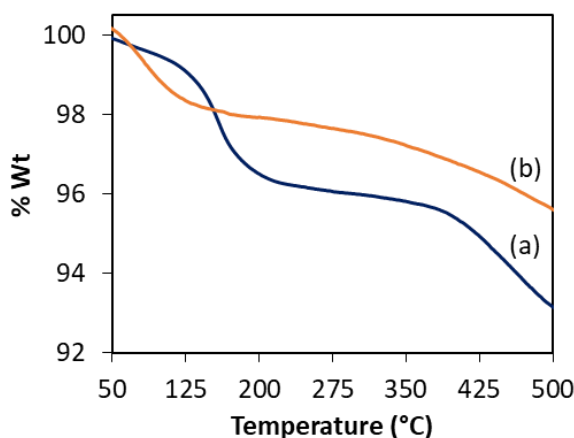


**Figure 4** TGA curves of (a) PdTPA and (b) PdTPA/SiO<sub>2</sub>.

The BET surface area of SiO<sub>2</sub> and PdTPA/SiO<sub>2</sub> were found to be 423 m<sup>2</sup>/g and 322 m<sup>2</sup>/g, respectively. The decrease in specific surface area is the first indication of the encapsulation of PdTPA into the pores of the SiO<sub>2</sub> via strong interaction. The N<sub>2</sub> physisorption isotherms (Figure 5) are of type IV in nature according to the IUPAC classification with an H1 hysteresis loop, a characteristic of mesoporous solids. Almost the same nature of the isotherms indicates the encapsulation of PdTPA inside the pores without any alteration of the structure, further, it was confirmed by FT-IR.

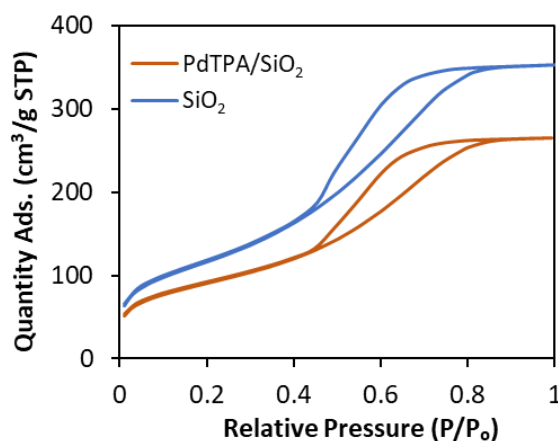


**Figure 5** Nitrogen physisorption isotherms.

FT-IR spectra of SiO<sub>2</sub>, TPA, PdTPA and PdTPA/SiO<sub>2</sub> are shown in figure 6. SiO<sub>2</sub> (Figure 6a) shows broad band in the region of 1300–1000, 966, 801, 458 cm<sup>-1</sup>

corresponding to asymmetric stretching of Si-O-Si, symmetric stretching of Si-OH, symmetric stretching and bending vibration of Si-O-Si, respectively. The characteristic bands for TPA (Figure 6b) are obtained at 1088, 987, 893 and 800  $\text{cm}^{-1}$  corresponding to P-O, W=O and W-O-W stretching, respectively. The characteristic bands for PdTPA (Figure 6c) are observed at 1080, 982, 890 and 795  $\text{cm}^{-1}$  corresponding to P-O, W=O, and W-O-W stretching, respectively. Here, no splitting of  $\nu(\text{P-O})$  into 1088 and 1042  $\text{cm}^{-1}$  confirms the presence of Pd as a counter ion only [13]. The slight shift in the  $\nu(\text{P-O})$  as compared to TPA may be due to the replacing of protons by Pd. The FT-IR spectrum of PdTPA/SiO<sub>2</sub> (Figure 6d) is almost identical to that of SiO<sub>2</sub>. The absence of respective P-O and W-O-W stretching may be due to the overlapping of bands with that of support, however, W=O stretching band was observed at 893  $\text{cm}^{-1}$  without any significant shift. The obtained results confirm the encapsulation of PdTPA into silica pores.

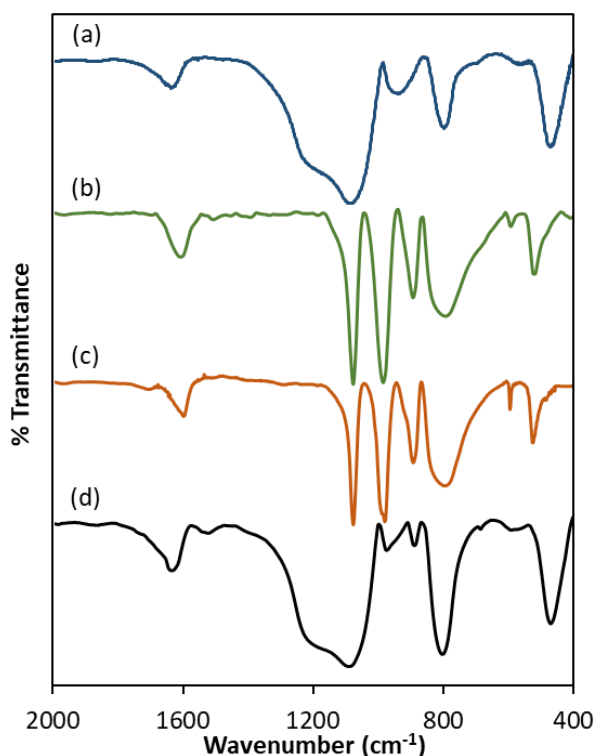


**Figure 6** FT-IR spectra of (a) SiO<sub>2</sub> (b) TPA (c) PdTPA and (d) PdTPA/SiO<sub>2</sub>.

$^{31}\text{P}$  MAS NMR is an important tool to understand the chemical environment around phosphorus in polyoxometalates as well as the interaction of the anion with support [14].  $^{31}\text{P}$  MAS NMR spectra of TPA, PdTPA and PdTPA/ $\text{SiO}_2$  are presented in figure 7. Pure TPA shows a single peak at -15.62 ppm and it is in good agreement with the reported one [15]. Whereas PdTPA shows an intense peak at -14.31 ppm, the observed low shift indicates that there is no significant effect of Pd on the electronic environment of phosphorus in TPA. In the case of PdTPA/ $\text{SiO}_2$ , observed shift at -13.97 ppm may be due to encapsulation of PdTPA into the pores of  $\text{SiO}_2$  by strong interaction [16], i.e. hydrogen bond. The obtained value was different from the reported chemical shifts for  $\text{PW}_{11}$  (-11.3 ppm) [17], confirming the absence of any lacunary structure as well as the presence of Pd as a counter ion only.

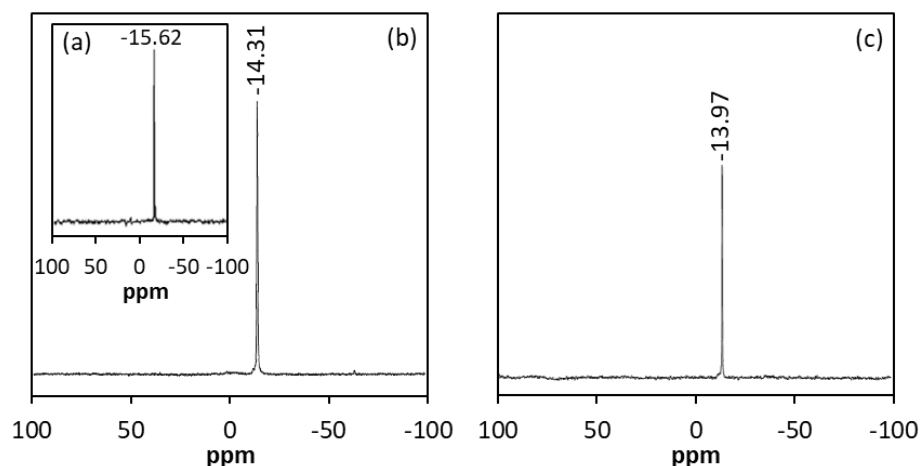


**Figure 7**  $^{31}\text{P}$  MAS NMR spectra of (a) TPA (inset), (b) PdTPA and (c) PdTPA/ $\text{SiO}_2$ .

To check the high degree of dispersion, XRD patterns of TPA, PdTPA,  $\text{SiO}_2$  and PdTPA/ $\text{SiO}_2$  were recorded (Figure 8). XRD pattern of the PdTPA shows all the patterns corresponds to TPA, indicating the retention of TPA structure. Moreover, four additional reflections are observed at  $2\theta$  of 38.5, 47.3, 59.8 and 68.1 that could be attributed to 111, 200, 220 and 311 planes of elemental palladium.  $\text{SiO}_2$  shows broad and flat diffraction peak with Bragg angle at  $2\theta$  of  $23^\circ$ , representing the amorphous nature of silica, in good agreement with the

reported one [18, 19]. Whereas, in XRD patterns of PdTPA/SiO<sub>2</sub>, absence of any crystalline peak corresponds to PdTPA, reveals the encapsulation of PdTPA with high dispersion of the material, inside the pores of SiO<sub>2</sub>. Here also, three additional reflections were observed at  $2\theta$  of 39.4, 46.7 and 59.8 attributed to 111, 200 and 220 planes of elemental palladium, indicating the retention of the cubic structure of palladium even after encapsulation into the silica pores. The reflection corresponding to the 311 plane was not clearly visible due to the noisy pattern. The presence of reflections corresponding to Pd and absence of crystalline peaks of TPA is the first indication of uniform dispersed Pd into the pores of silica.

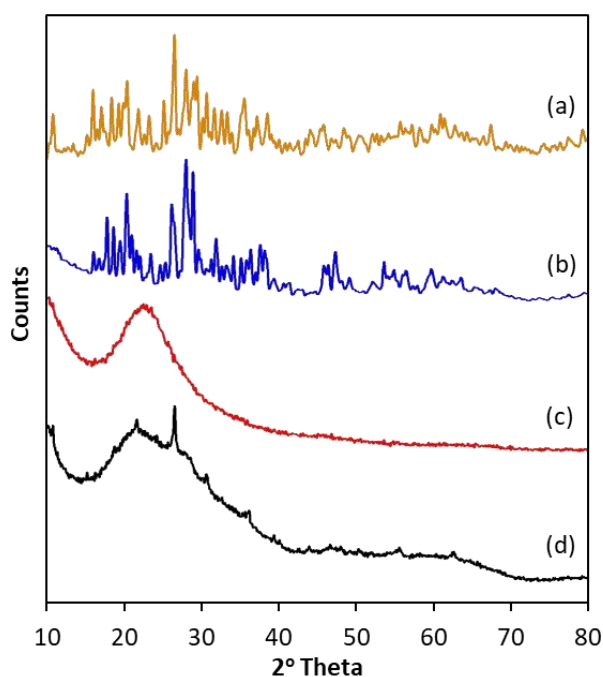


**Figure 8** XRD pattern of (a) TPA, (b) PdTPA, (c) SiO<sub>2</sub> and (d) PdTPA/SiO<sub>2</sub>.

To confirm the electronic properties of Pd and W, the XPS spectra of PdTPA and PdTPA/SiO<sub>2</sub> were recorded (Figure 9). Both the catalysts show a very intense peak at binding energy 532 eV (Pd3p<sub>3/2</sub> and O1s) as they contain PdTPA precursor and SiO<sub>2</sub> as the carrier, which is in good agreement with the well-known fact that there is direct overlap between Pd3p<sub>3/2</sub> and O1s peaks [20], and cannot be assigned to confirm the presence of Pd(0). Hence, we have presented

instrument generated full spectra (Figure 9a & 9d) images supporting the presence of Pd(0). This was further confirmed by recording the high resolution Pd3d and W4f XPS spectra of both the materials.

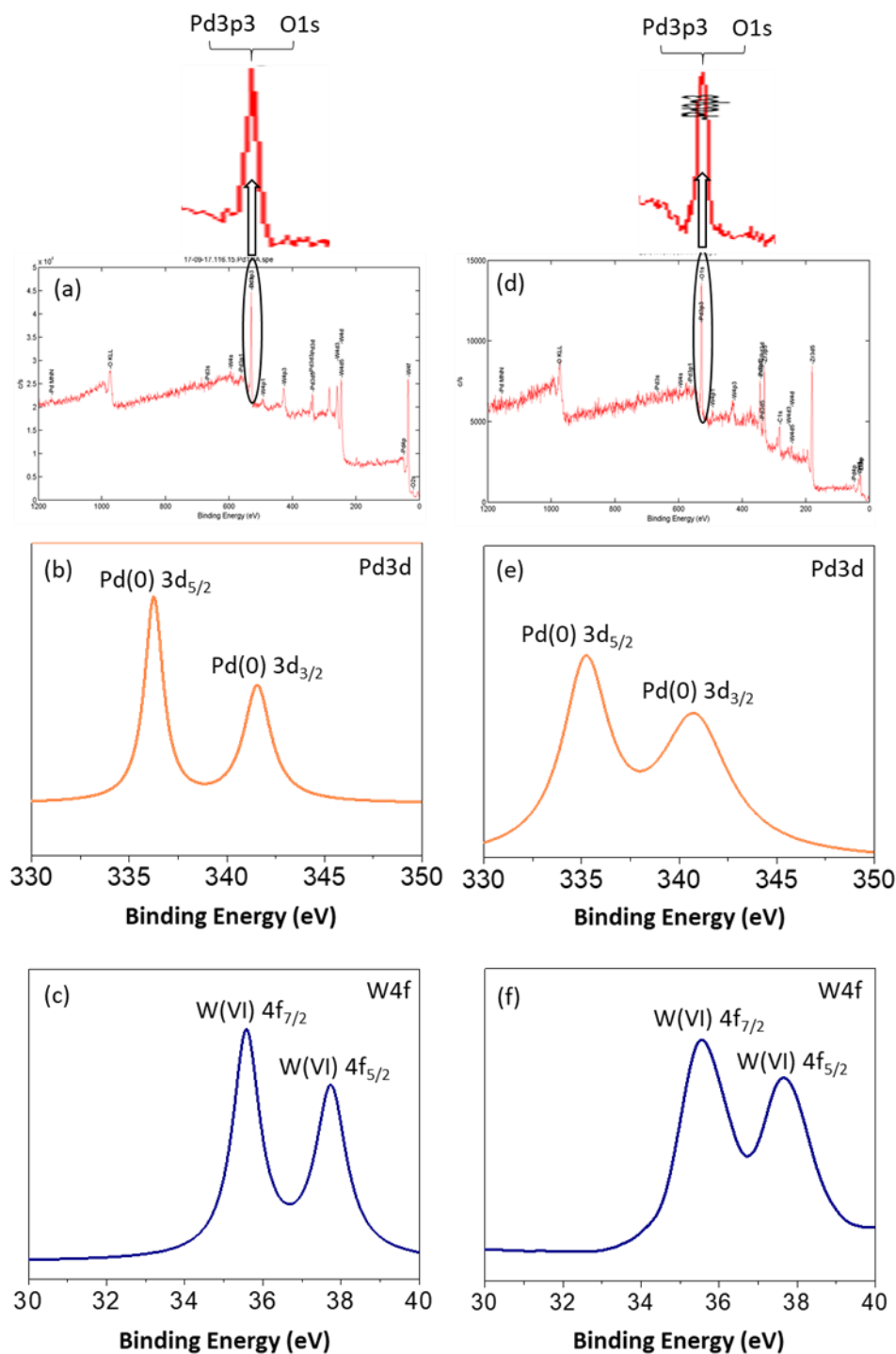


**Figure 9** XPS spectra of PdTPA (a, b and c) and PdTPA/SiO<sub>2</sub> (d, e and f).



PdTPA shows a spin orbit doublet peak of Pd3d at binding energy 335.9 eV ( $3d_{5/2}$ ) and 340.9 eV ( $3d_{3/2}$ ), confirming the presence of Pd(0) [21-24]. Similarly, PdTPA/SiO<sub>2</sub> reflects the same at 335.7 eV ( $3d_{5/2}$ ) and 340.7 eV ( $3d_{3/2}$ ), indicating the presence of the Pd(0) in to the encapsulated material.

The W4f peak was composed of a well resolved spin orbit doublet (35.6 eV and 37.8 eV for PdTPA, 35.5 eV and 37.7 eV for PdTPA/SiO<sub>2</sub> correspond to W4f<sub>7/2</sub> and W4f<sub>5/2</sub>, respectively), typical of W(VI), in agreement with literature data on Keggin-type POMs [22,25], confirming no reduction of W(VI) during the synthesis of material.

TEM images of PdTPA, SiO<sub>2</sub> and PdTPA/SiO<sub>2</sub> are presented (Figure 10a-d) at various magnifications. Image 10a (PdTPA) clearly shows the presence of very tiny Pd(0) nanoclusters throughout the morphology without any aggregates formation, confirming the stabilization of PdNCLs by TPA. Images 10(c-d) (PdTPA/SiO<sub>2</sub>) shows the encapsulation of PdTPA, confirming the presence of homogeneously dispersed PdNCLs into the pores of SiO<sub>2</sub>. For more clarification, HRTEM images (Figure 10e-f) of PdTPA/SiO<sub>2</sub> were recorded, which clearly shows the uniform dispersion of isolated PdNCLs (~2 nm and less) inside the pores of SiO<sub>2</sub> without any aggregation.

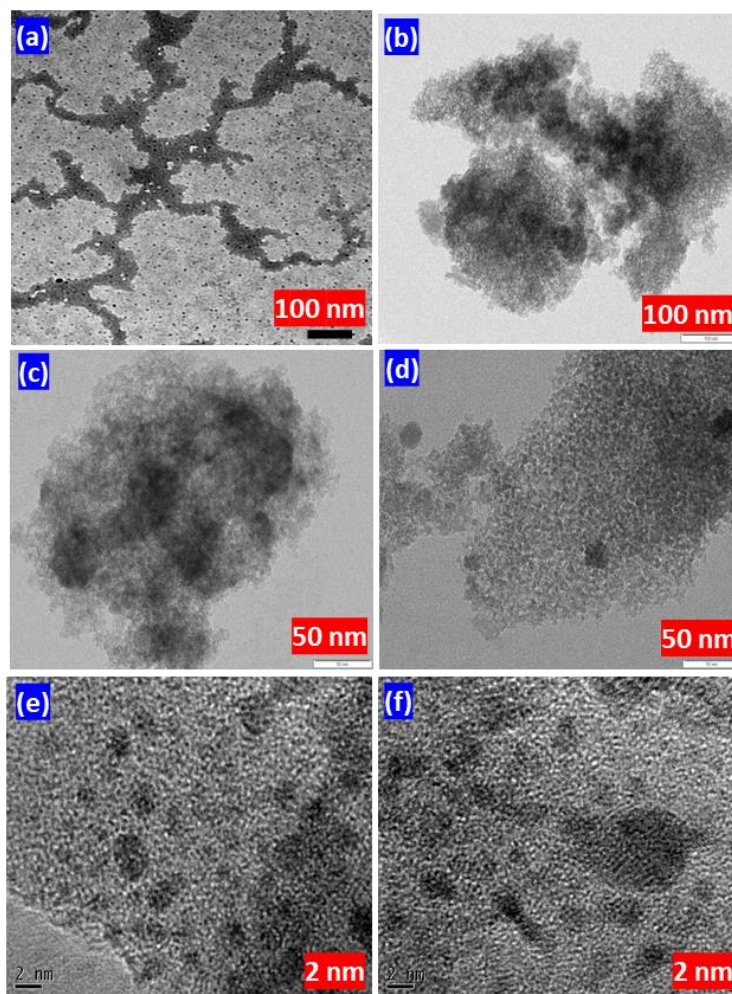


**Figure 10** TEM micrographs of (a) PdTPA, (b) SiO<sub>2</sub>, (c & d) PdTPA/SiO<sub>2</sub> and HRTEM micrographs of (e & f) PdTPA/SiO<sub>2</sub>.

The sole presence of isolated PdNCLs was confirmed by STEM (figure 11). Image 11a as well as 11b highlights the presence of isolated PdNCLs sites (bright field; as dark black spots and dark field; white spots, respectively) with homogeneous distribution, almost having the equal nearest-neighboring distance inside the pores of silica support. Whereas, overlapping image (Figure 11c) as well as elemental image of Pd (Figure 11d) clearly indicates the presence of isolated PdNCLs homogeneously dispersed without any cross talks between them. Elemental images (11d-h) show the presence of all the possible elements in the synthesized catalyst. TEM, HRTEM and STEM combinedly expose the homogeneous encapsulation of PdNCLs into the pores of the SiO<sub>2</sub>. Noticeably,

no aggregates formation of Pd was observed throughout the morphology indicates the stabilization of Pd by TPA.

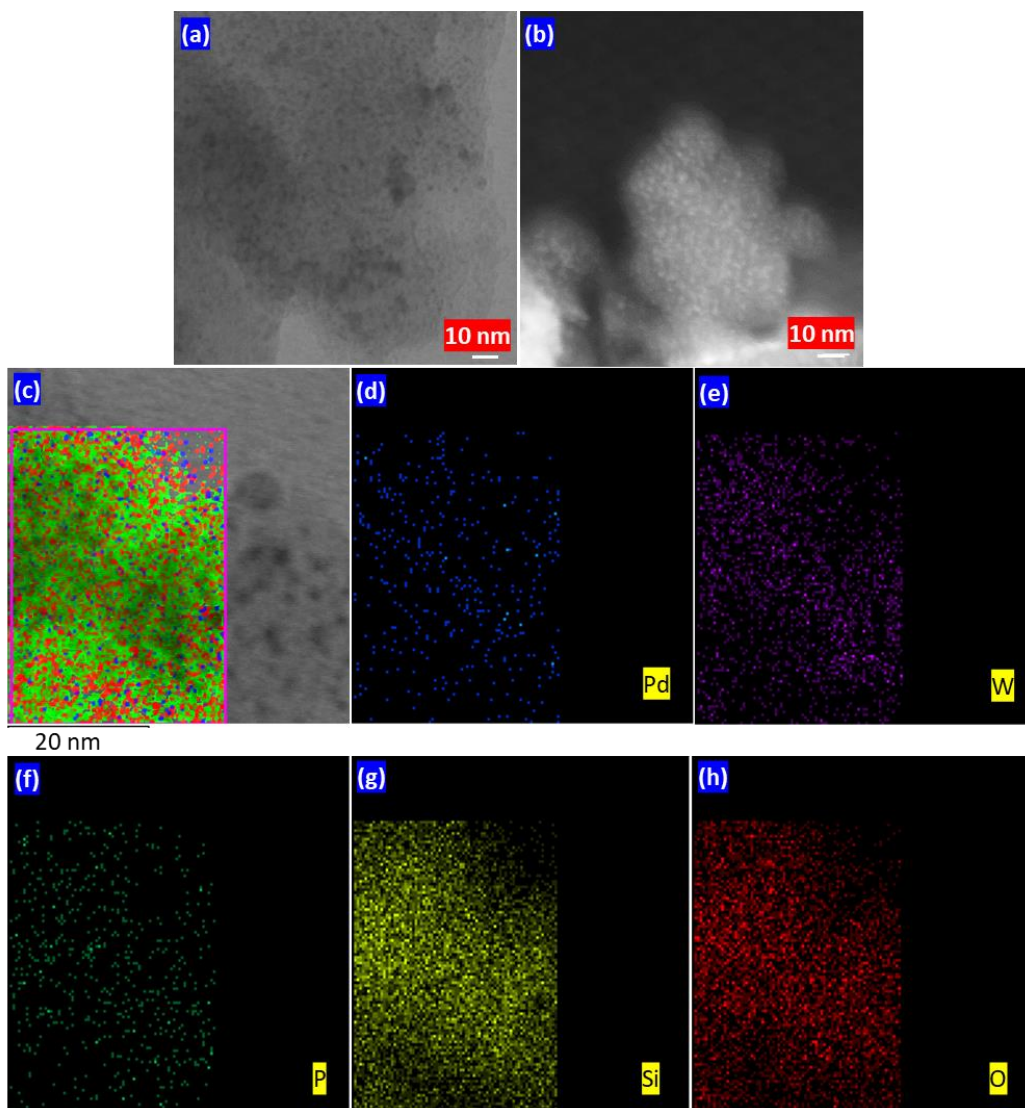


**Figure 11** (a) Bright field, (b) dark field STEM images of PdTPA/SiO<sub>2</sub>. (c) Overlapping, (d-h) elemental images of PdTPA/SiO<sub>2</sub>.

In summary, FT-IR and <sup>31</sup>P MAS NMR data show the presence of palladium as a counter ion only without degradation of TPA structure even after encapsulation into the SiO<sub>2</sub>. The presence of Pd(0) and W(VI) were confirmed by XPS. TEM, HRTEM and STEM confirmed homogeneous dispersion of PdNCLs into the SiO<sub>2</sub>.

## Catalytic activity

### SM Coupling

To evaluate the efficiency of the catalyst for SM coupling, iodobenzene (1.96 mmol) and phenylboronic acid (2.94 mmol) were selected as test substrates. Effect of different reaction parameters such as palladium concentration, time, temperature, base, solvent and solvent ratio were studied to optimize the conditions for maximum conversion (Figure 12).

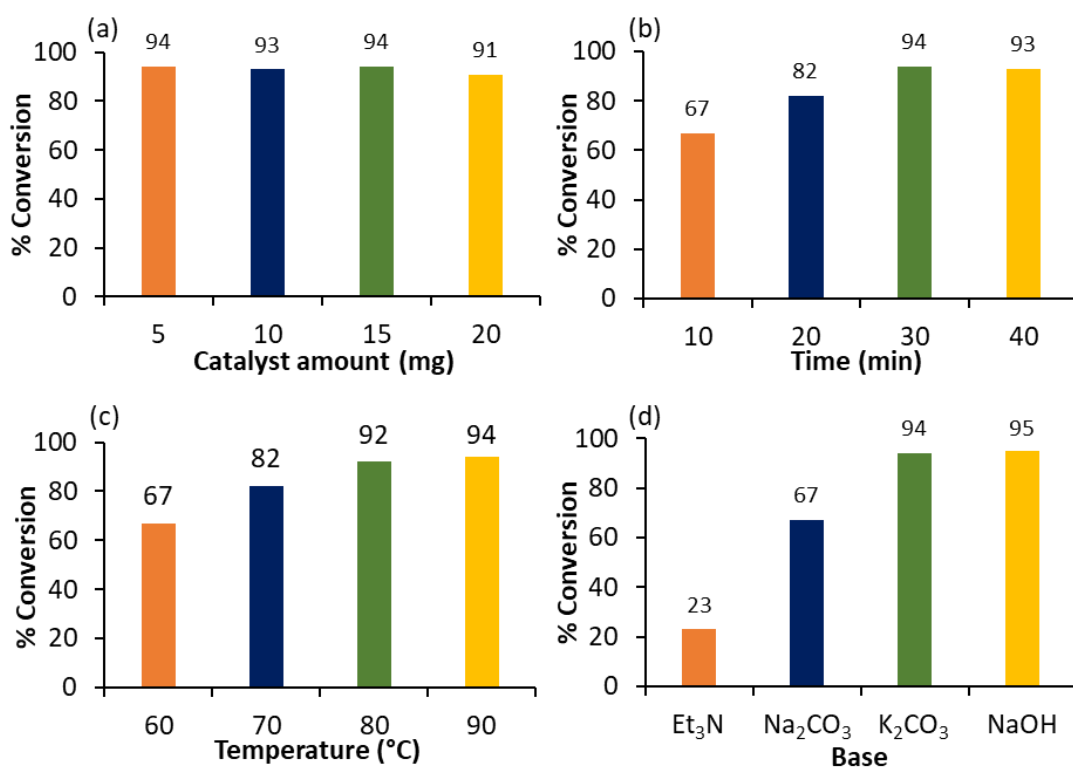


**Figure 12** Optimization of parameters for SM coupling. Reaction conditions: (a) Effect of catalyst amount- K<sub>2</sub>CO<sub>3</sub> (3.92 mmol), EtOH: H<sub>2</sub>O (3:7 mL), time (30 min), temperature (90 °C); (b) Effect of time- catalyst (5 mg), K<sub>2</sub>CO<sub>3</sub> (3.92 mmol), EtOH: H<sub>2</sub>O (3:7 mL), temperature (90 °C); (c) Effect of temperature- catalyst (5 mg), K<sub>2</sub>CO<sub>3</sub> (3.92 mmol), EtOH: H<sub>2</sub>O (3:7 mL), time (30 min); (d) Effect of base- catalyst (5 mg), base (3.92 mmol), EtOH: H<sub>2</sub>O (3:7 mL), time (30 min), temperature (90 °C).

As discussed in earlier chapters, we have screened the all parameters thoroughly to achieve maximum % conversion. It should be noted that the explanation will remain the same. Obtained results are presented in figure 12, table 1 & 2.

**Table 1** Effect of solvent

Solvent	% Conversion
Toluene	17
Acetonitrile	28
Ethanol	68
H <sub>2</sub> O	32

Reaction conditions: Catalyst (5 mg), K<sub>2</sub>CO<sub>3</sub> (3.92 mmol), solvent (10 mL), time (30 min), temperature (90 °C).

**Table 2** Effect of solvent ratio

Ethanol: H <sub>2</sub> O	% Conversion
1:9	77
2:8	83
3:7	94
4:6	94
5:5	93

Reaction conditions: Catalyst (5 mg), K<sub>2</sub>CO<sub>3</sub> (3.92 mmol), time (30 min), temperature (90 °C).

From the above study, the optimized conditions for the maximum % conversion (94) are: iodobenzene (1.96 mmol), phenylboronic acid (2.94 mmol), K<sub>2</sub>CO<sub>3</sub> (3.92 mmol), conc. of Pd ( $3.76 \times 10^{-4}$  mmol, 0.0192 mol%), substrate/catalyst ratio (5215/1), C<sub>2</sub>H<sub>5</sub>OH:H<sub>2</sub>O (3:7 mL), time (30 min), temperature (90 °C). The calculated TON is 4902 and TOF is 9804 h<sup>-1</sup>.

## Heck coupling

To evaluate the efficiency of the catalyst for heck coupling, iodobenzene (0.98 mmol) and styrene (1.47 mmol) were selected as test substrates. Effect of different reaction parameters such as palladium concentration, time, temperature, base, solvent and solvent ratio was studied to optimize the conditions for maximum conversion. Obtained results are shown in figure 13, table 3 and table 4.

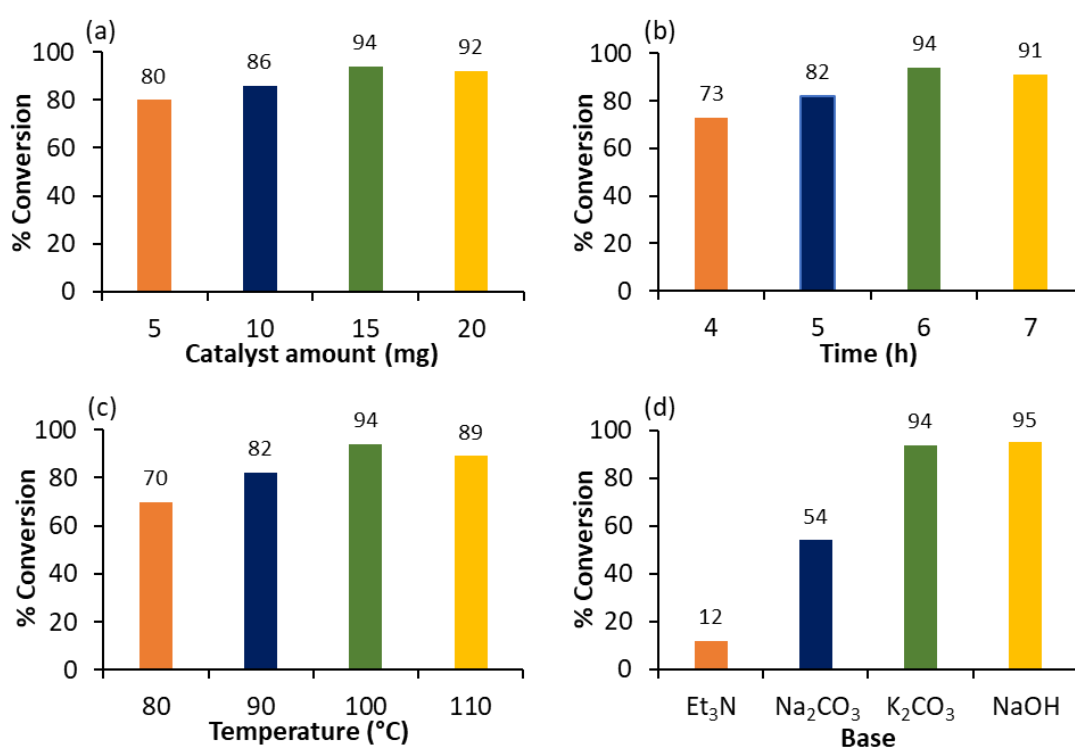


**Figure 13** Optimization of Heck coupling. Reaction conditions: (a) Effect of catalyst amount- K<sub>2</sub>CO<sub>3</sub> (1.96 mmol), DMF:H<sub>2</sub>O (3:2 mL), time (6 h), temperature (100 °C); (b) Effect of time- catalyst (15 mg), K<sub>2</sub>CO<sub>3</sub> (1.96 mmol), DMF:H<sub>2</sub>O (3:2 mL), temperature (100 °C), (c) Effect of temperature- catalyst (15 mg), K<sub>2</sub>CO<sub>3</sub> (1.96 mmol), DMF:H<sub>2</sub>O (3:2 mL), time (6 h); (d) Effect of base- catalyst (15 mg), base (1.96 mmol), DMF:H<sub>2</sub>O (3:2 mL), time (6 h), temperature (100 °C).

**Table 3** Effect of solvent

Solvent	% Conversion
Toluene	5
Ethanol	25
DMF	75
H <sub>2</sub> O	2

Reaction conditions: Catalyst (15 mg), K<sub>2</sub>CO<sub>3</sub> (1.96 mmol), time (6 h), temperature (100 °C).

**Table 4** Effect of solvent ratio

DMF: H <sub>2</sub> O	% Conversion
1:4	27
2:3	40
3:2	94
4:1	86

Reaction conditions: Catalyst (15 mg), K<sub>2</sub>CO<sub>3</sub> (1.96 mmol), time (6 h), temperature (100 °C).

The optimized conditions for the maximum % conversion (94) are: iodobenzene (0.98 mmol), styrene (1.47 mmol), K<sub>2</sub>CO<sub>3</sub> (1.96 mmol), conc. of Pd ( $1.13 \times 10^{-3}$  mmol, 0.115 mol%), substrate/catalyst ratio (869/1), DMF:H<sub>2</sub>O (3:2 mL), time (6 h), temperature (100 °C). The calculated turnover number (TON) is 817 and turnover frequency (TOF) is 136 h<sup>-1</sup>.

## Hydrogenation

To evaluate the efficiency of the catalyst for hydrogenation, cyclohexene (9.87 mmol) was selected as test substrate. Effect of different reaction parameters such as palladium concentration, time, temperature, pressure and solvent were studied to optimize the conditions for maximum conversion. Obtained results are shown in figure 14 and table 5.

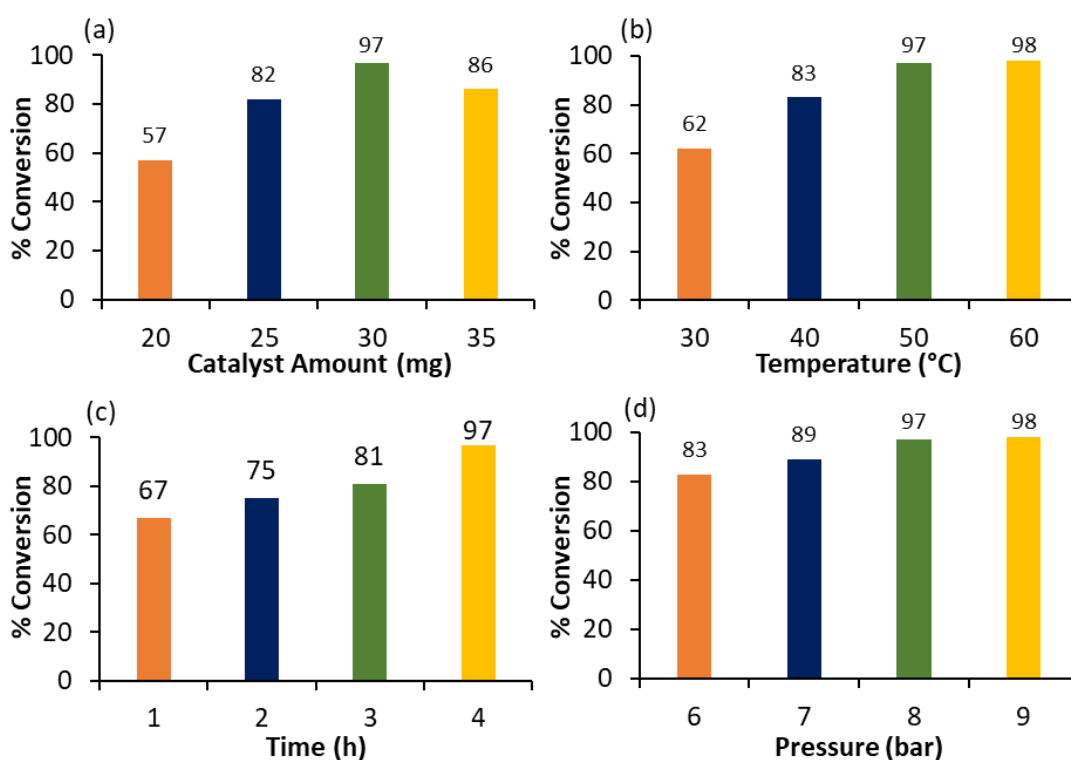


**Figure 14** Optimization of cyclohexene hydrogenation. Reaction conditions: (a) Effect of catalyst amount- cyclohexene (9.87 mmol), H<sub>2</sub>O (50 mL), time (4 h), temperature (80 °C), H<sub>2</sub> pressure (10 bar); (b) Effect of temperature- cyclohexene (9.87 mmol), H<sub>2</sub>O (50 mL), catalyst (30 mg), time (4 h), H<sub>2</sub> pressure (10 bar); (c) Effect of time: cyclohexene (9.87 mmol), H<sub>2</sub>O (50 mL), catalyst (30 mg), temperature (50 °C), H<sub>2</sub> pressure (10 bar); (d) Effect of pressure: cyclohexene (9.87 mmol), H<sub>2</sub>O (50 mL), catalyst (30 mg), time (4 h), temperature (50 °C).



**Table 5** Effect of solvent

Solvent (20: 30) mL	% Conversion
CH <sub>3</sub> CN: H <sub>2</sub> O	79
IPA: H <sub>2</sub> O	92
EtOH: H <sub>2</sub> O	96
H <sub>2</sub> O (50 mL)	97

Reaction conditions: cyclohexene (9.87 mmol), catalyst (30 mg), time (4 h), temperature (50 °C), H<sub>2</sub> pressure (8 bar).

The optimized conditions for the maximum % conversion (97) are: cyclohexene (9.87 mmol), H<sub>2</sub>O (50 mL), conc. of Pd ( $1.50 \times 10^{-3}$  mmol, 0.023 mol%), substrate/catalyst ratio (4377/1), time (4 h), temperature (50 °C) and H<sub>2</sub> pressure (8 bar). The calculated TON is 4245 and TOF is 1061 h<sup>-1</sup>.

## Control Experiments

In all the three reactions, control experiments were carried out with TPA, SiO<sub>2</sub>, PdCl<sub>2</sub> and PdTPA under optimized conditions in order to understand the role of each component and results are shown in table 6. It is seen from the table that TPA and SiO<sub>2</sub> were inactive towards the reactions. Whereas significant conversion was found in the case of PdCl<sub>2</sub>, PdTPA and PdTPA/SiO<sub>2</sub> in all reactions. This indicates that Pd is real active species responsible for the reactions.

**Table 6** Control experiment

Catalyst	SM	Heck	Hydrogenation
	% Conversion <sup>a</sup>	% Conversion <sup>b</sup>	% Conversion <sup>c</sup>
TPA ( <sup>a</sup> 1.15, <sup>b</sup> 3.46, <sup>c</sup> 6.92 mg)	N. R.	N. R.	N. R.
SiO <sub>2</sub> ( <sup>a</sup> 3.85, <sup>b</sup> 11.54, <sup>c</sup> 23.08 mg)	N. R.	N. R.	N. R.
PdCl <sub>2</sub>	99	96	86
PdTPA	96	96	88
PdTPA/SiO <sub>2</sub>	94	94	97

Reaction conditions. (a) *SM coupling*: iodobenzene (1.96 mmol), phenylboronic acid (2.94 mmol), catalyst (0.04 mg Pd, 0.0192 mol% Pd), K<sub>2</sub>CO<sub>3</sub> (3.92 mmol), C<sub>2</sub>H<sub>5</sub>OH: H<sub>2</sub>O (3:7 mL), time (30 min), temperature (90 °C); (b) *Heck coupling*: iodobenzene (0.98 mmol), styrene (1.47 mmol), catalyst (0.12 mg Pd, 0.115 mol% Pd), K<sub>2</sub>CO<sub>3</sub> (1.96 mmol), DMF: H<sub>2</sub>O (3:2 mL), time (6 h), temperature (100 °C); (c) *Hydrogenation*: cyclohexene (9.87 mmol), catalyst (0.24 mg Pd, 0.023 mol% Pd), H<sub>2</sub>O (50 mL), time (4 h), temperature (50 °C), H<sub>2</sub> pressure (8 bar). N. R. - No reaction.

## Leaching and Heterogeneity test

The leaching of PdNCLs as well as TPA from SiO<sub>2</sub> was checked following the same method as discussed in chapter-2 (Please refer, Page No. 204-205) and found no leaching of either Pd or TPA from SiO<sub>2</sub>. However, the minor change in % conversion (Table 7) may be due to the instrument error ( $\pm 1-1.5$  %). Like in case of PdTPA/ZrO<sub>2</sub> (Chapter-2), in the present case, it was also found that SiO<sub>2</sub> holds PdTPA very strongly and does not allow to leach it into the reaction mixture, making it a true heterogeneous catalyst of category C [26].

Table 7 Leaching test

Catalyst	SM	Heck	Hydrogenation
	% Conversion <sup>a</sup>	% Conversion <sup>b</sup>	% Conversion <sup>c</sup>
PdTPA/SiO <sub>2</sub>	67 (after 10 min)	65 (after 3 h)	75 (after 2 h)
	66 (after 30 min)	65 (after 6 h)	76 (after 4 h)

Leaching test. Reaction conditions. (a) *SM coupling*: iodobenzene (1.96 mmol), phenylboronic acid (2.94 mmol), catalyst (0.04 mg Pd, 0.0192 mol% Pd), K<sub>2</sub>CO<sub>3</sub> (3.92 mmol), C<sub>2</sub>H<sub>5</sub>OH: H<sub>2</sub>O (3:7 mL), temperature (90 °C); (b) *Heck coupling*: iodobenzene (0.98 mmol), styrene (1.47 mmol), catalyst (0.12 mg Pd, 0.115 mol% Pd), K<sub>2</sub>CO<sub>3</sub> (1.96 mmol), DMF: H<sub>2</sub>O (3:2 mL), temperature (100 °C); (c) *Hydrogenation*: cyclohexene (9.87 mmol), catalyst (0.24 mg Pd, 0.023 mol% Pd), H<sub>2</sub>O (50 mL), temperature (50 °C), H<sub>2</sub> pressure (8 bar).

## Recyclability and sustainability of the catalyst

Recyclability and sustainability for PdTPA and PdTPA/SiO<sub>2</sub> were studied as described in chapter-2 (Please refer, Page No. 206-207) and the results are described in figure 15. Obtained results show that, while PdTPA exhibited gradual decrease in % conversion due to leaching of active PdNCLs, PdTPA/SiO<sub>2</sub> displayed constant % conversion up to five cycles for all reactions, as in case of PdTPA/ZrO<sub>2</sub> thereby confirming the important role played by the support.

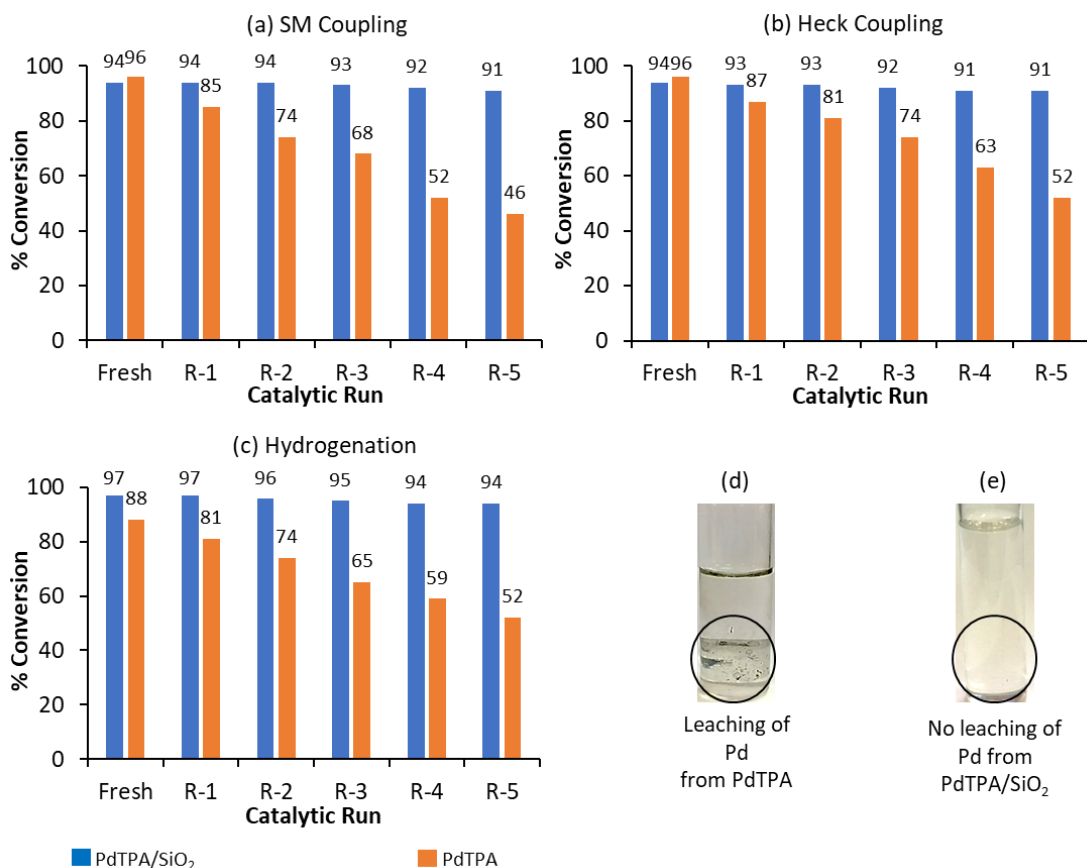


**Figure 15** Recycling test. Reaction conditions: (a) *SM coupling*- iodobenzene (1.96 mmol), phenylboronic acid (2.94 mmol), catalyst (0.04 mg Pd, 0.0192 mol% Pd), K<sub>2</sub>CO<sub>3</sub> (3.92 mmol), C<sub>2</sub>H<sub>5</sub>OH: H<sub>2</sub>O (3:7 mL), time (30 min), temperature (90 °C); (b) *Heck coupling*- iodobenzene (0.98 mmol), styrene (1.47 mmol), catalyst (0.12 mg Pd, 0.115 mol% Pd), K<sub>2</sub>CO<sub>3</sub> (1.96 mmol), DMF: H<sub>2</sub>O (3:2 mL), time (6 h), temperature (100 °C); (c) *Hydrogenation*- cyclohexene (9.87 mmol), catalyst (0.24 mg Pd, 0.023 mol% Pd), H<sub>2</sub>O (50 mL), time (4 h), temperature (50 °C), H<sub>2</sub> pressure (8 bar); (d) Leaching of Pd from PdTPA during the reaction and (e) No leaching of Pd from PTPA/SiO<sub>2</sub> during the reaction.

### Characterization of regenerated catalyst

In order to check the stability, regenerated catalyst was characterized by EDX, BET, FT-IR, XPS and TEM.

EDX values of Pd (0.79 wt%) and W (16.32 wt%) of regenerated PdTPA/SiO<sub>2</sub> (Figure 16) is in good agreement with values of fresh catalyst (0.80 wt% of Pd, 16.43 wt% of W) confirming no emission of Pd and TPA from SiO<sub>2</sub> during the reaction.

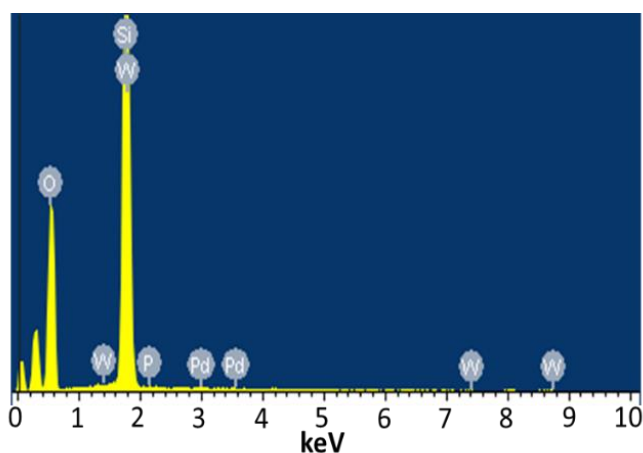


**Figure 16** EDX mapping of regenerated PdTPA/SiO<sub>2</sub>.

Identical BET surface area of fresh (320 m<sup>2</sup>/g) and regenerated (318 m<sup>2</sup>/g) catalysts indicates that PdNCLs sites remains intact during the reaction, do not undergo sintering or aggregation. Moreover, no change in N<sub>2</sub> sorption isotherms (Figure 17) of regenerated one proved that surface phenomena as well as bulk (pores) remains intact. This result can be seen in TEM also.

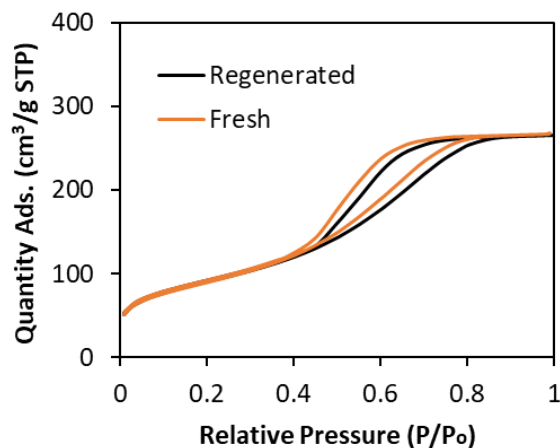


**Figure 17** N<sub>2</sub> Sorption Isotherms.

The FT-IR spectra of the fresh and regenerated catalyst are shown in figure 18. From the spectra it can be seen that almost identical spectrum was obtained without any significant shift in characteristic bands of regenerated catalyst compare to fresh catalyst, indicate that catalyst structure remained unaltered even after the regeneration. However, the spectrum was slightly different in terms of intensity. This might be due to the sticking of the substrates on the surface, although this might not be significant in the reutilization of the catalyst [27].

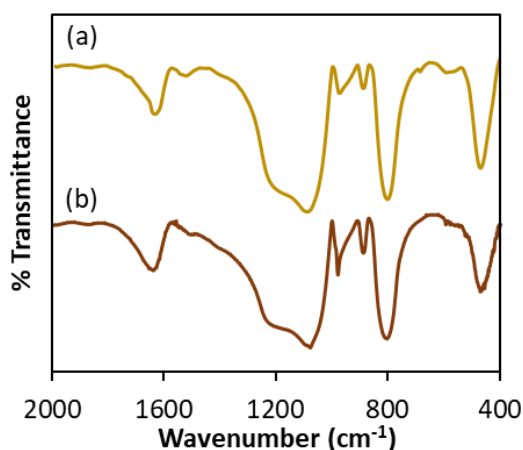


**Figure 18** FT-IR spectra of (a) fresh and (b) regenerated PdTPA/SiO<sub>2</sub>.

XPS spectra of regenerated PdTPA/SiO<sub>2</sub> are displayed in figure 19. The spectra of regenerated catalyst were found to be identical with fresh one (Figure 8),

confirm the retention of Pd active as well as W(VI), which do not undergo reduction during the hydrogenation reaction, indicating the sustainability of the catalyst.

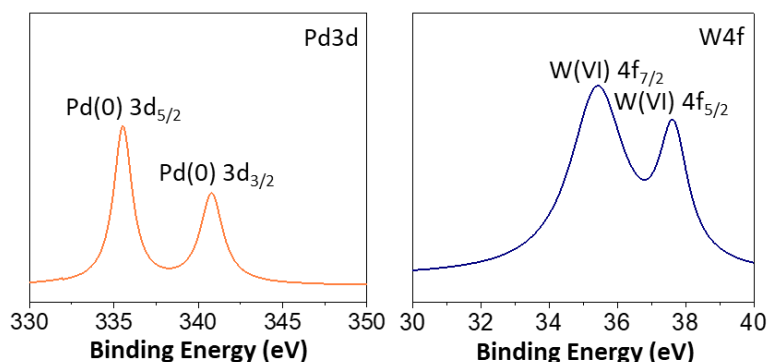


**Figure 19** XPS spectra of regenerated PdTPA/SiO<sub>2</sub>.

TEM micrographs of regenerated catalyst are presented in figure 20, clearly show the retention of the homogeneously dispersed PdNCLs, confirming the stability and sustainability of the catalyst.

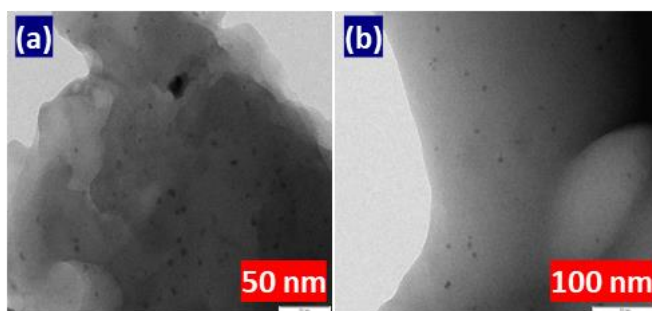


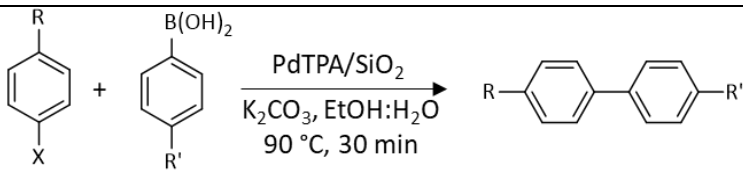
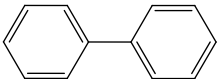
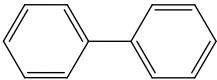
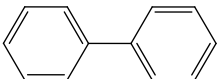
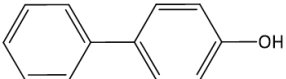
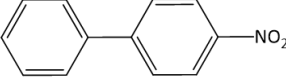
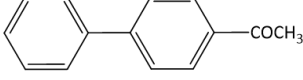
**Figure 20** TEM images of Regenerated Pd-TPA/SiO<sub>2</sub>.

In conclusion, FT-IR shows the retention of TPA structure even after its reuse number of times. XPS and TEM confirm the presence of homogeneously dispersed PdNCLs sites inside the cavity of the SiO<sub>2</sub>. While BET surface area and N<sub>2</sub> sorption curves reveal the unaltered uniform encapsulated dispersion of PdNCLs inside the pores of SiO<sub>2</sub>.

### Scope for Catalysis

Under the optimized condition, the scope and limitations of substrates were investigated for SM coupling by using different halobenzenes (Table 8) and the similar trend of the activity was found as discussed in the earlier chapters.

**Table 8** Substrate study for SM coupling

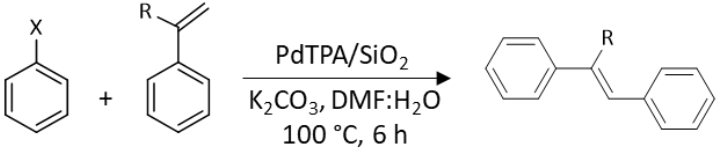
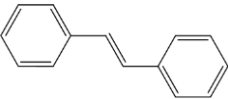
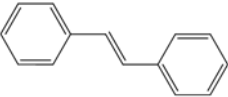
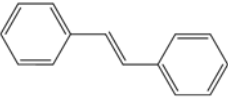
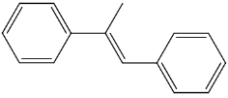
					
R	X	R'	Product	% Conversion	TON/TOF (h <sup>-1</sup> )
H	I	H		94	4902/9804
H	Br	H		58	3024/6048
				86 (5 h)	4485/897
H	Cl	H		4	209/418
				74 (10 h)	3859/386
OH	Br	H		88	4589/9178
NO <sub>2</sub>	Br	H		92	4797/9594
COCH <sub>3</sub>	Br	H		81	4224/8448

Reaction conditions: Halobenzene (1.96 mmol), phenylboronic acid (2.94 mmol), K<sub>2</sub>CO<sub>3</sub> (3.92 mmol), conc. of Pd(0) (0.0192 mol%), substrate/catalyst ratio (5215/1), C<sub>2</sub>H<sub>5</sub>OH: H<sub>2</sub>O (3:7) mL, 30 min, 90 °C.



Similarly, under optimized conditions, scope and limitations of substrates for Heck coupling were also investigated by using different halobenzenes and styrene derivatives, the obtained results are presented in table 9.

**Table 9** Substrate study for Heck coupling

				
X	R	Product	% Conversion	TON/TOF (h <sup>-1</sup> )
I	H		94	817/136
Br	H		52 81*	452/75 704*/70*
Cl	H		10 51*	87/14 443*/44*
I	CH <sub>3</sub>		61 82*	530/88 713*/71*

Reaction conditions: Halobenzene (0.98 mmol), styrene (1.47 mmol), K<sub>2</sub>CO<sub>3</sub> (1.96 mmol), conc. of Pd (0.115 mol%), substrate/catalyst ratio (869/1), DMF: H<sub>2</sub>O (3:2 mL), time (6 h), temperature (100 °C). \*Time (10 h).

Scope and limitation of the catalyst towards hydrogenation of substrates comprising of the different groups were evaluated such as alkene/arene, aldehyde, nitro and halogenated compounds (Table 10).

Selective C=C catalytic hydrogenation is a diverse and versatile acceptable route to synthesize precursors for various intermediates [28] and still, is a fascinating and challenging field. The efficiency of the catalyst was evaluated towards different aliphatic and aromatic alkenes, and achieved results summarize the viability of the catalyst for all types of alkenes (linear, aromatic and cyclic alkenes) using water as the solvent even though hydrophobic nature of all the

substrates. Ring size effect (Entry 1 & 2) and linear alkene chain effect (Entry 3 & 4) were observed for the activity of the catalyst. No substitution effect was observed on the conversion (Entry 5, 6 & 7). The present catalyst was found to be highly active for phenylacetylene, no partial hydrogenation was found (Entry 8). Moreover, the catalyst was found to be active for selective hydrogenation of the C=C bond without tolerating the C=O bond when simultaneously present in the substrates (Entry 10 & 11).

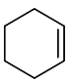
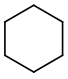
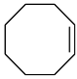
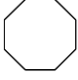
Catalytic hydrogenation of aldehydes is one of the most significant and widespread organic transformations due to formed product alcohol, offers great potential for acids, esters, acetals for perfume and pharmaceutical industries. A variety of substrates have been tolerated for hydrogenation and obtained results are tabulated. Entry 13, 14 and 15 show the positional isomer effect for bromobenzaldehyde and obtained moderate to excellent conversion indicated the catalyst activity order for  $p > o > m$  isomers. The catalyst was found inactive towards aliphatic aldehyde group such as crotonaldehyde (Entry 10), cinnamaldehyde (Entry 11), butyraldehyde and valeraldehyde. Achieved data summarize that the present catalyst can tolerate only the aldehyde group when it attached with aromatic ring directly, which could be a great tool for the synthesis of natural and pharmaceutical products selectively.



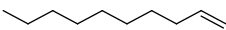
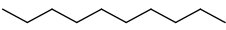
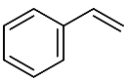
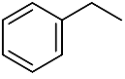
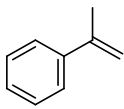
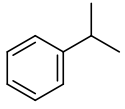
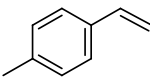
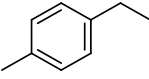
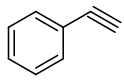
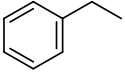
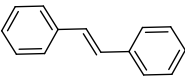
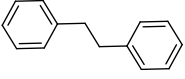
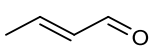
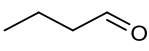
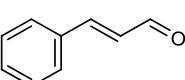
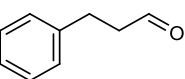
Catalytic hydrogenation of aromatic nitro compounds is an important process for the introduction of the amino group into pharmaceutical and agro-chemicals. Hydrogenation reaction of nitrobenzene, a relatively hard to hydrogenate [29]. To study the influence of the position of the electron releasing group in nitrobenzene for the hydrogenation, various isomers of nitrotoluenes were investigated. It was observed that the position of the electron releasing substituent in nitrobenzene exerts a remarkable influence on the activity of the catalyst. Among the nitrotoluenes, *o*- and *p*-isomers were hydrogenated faster than *m*-isomers (Entry 16-19). The effect of various electron-donating and withdrawing groups was also evaluated (Entry 20-24).

Hydrodehalogenation of aromatic halides, is a chemical transformation with important industrial applications for detoxification of halogenated aromatic wastes, is indeed an environmentally friendly and cost-saving alternative to their traditional disposal by incineration [30]. For this type of reaction in the liquid phase, it was general to select organic solvents as the reaction medium. HX derived from the reaction has been shown to inhibit the activity of Pd based catalyst [31]. To overcome from this base are generally used as proton scavenger, though formed NaX salt gets deposited on Pd based catalyst to cause deactivation [31].

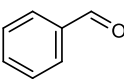
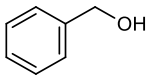
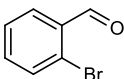
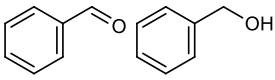
In the present case, we studied the same in water as solvent, proton scavenger free, without compromising the efficiency of the catalyst. *o*, *m* and *p*- positional effect were studied by bromobenzaldehyde isomers as model substrates. Entries 13, 14, & 15 show the activity order  $p > o > m$  isomers. Whereas, the effect of halo group showed the activity order  $\text{Br} > \text{Cl}$  (Entry 14 & 25). Entry 15 & 26 exposed the catalyst selective efficiency towards hydrodehalogenation of the substrate having keto group compared to aldehyde one. The reaction was found more feasible in the case of an electron releasing group compared to the withdrawing group (Entry 27 & 28). Obtained good to excellent conversion proved no deactivation of the catalyst by the formation of side product HX.

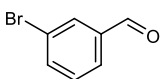
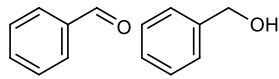
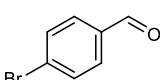
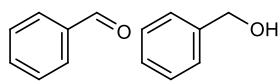
**Table 10** Substrate study for hydrogenation

Entry	Substrate	% Conversion/Selectivity	TON/TOF (h <sup>-1</sup> )
Alkene			
1		 97	4245/1061
2		 43	1882/471

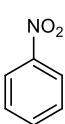
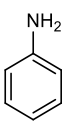
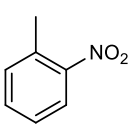
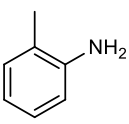
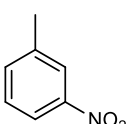
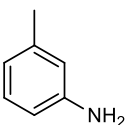
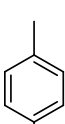
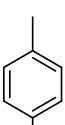
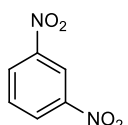
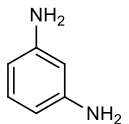
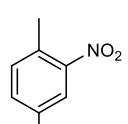
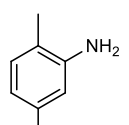
3		 54	2363/591
4		 67	2932/733
5		 98	4289/1072
6		 >99/100	4333/1083
7		 >99/100	4333/1083
8		 >99	4333/1083
9		 89	3895/974
10		 >99/100	4333/1083
11		 88/100	3851/963

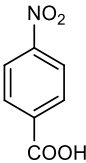
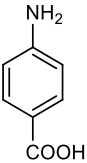
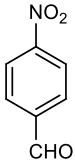
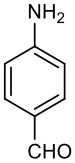
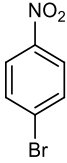
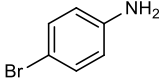
## Aldehydes

12		 37	1619/405
13		 89/68/32	3895/974

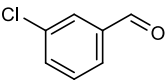
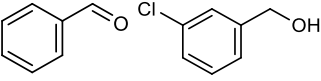
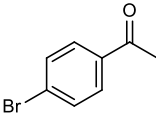
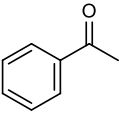
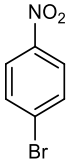
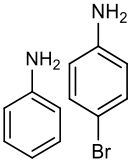
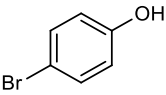
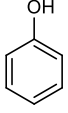
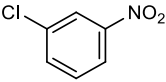
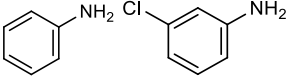
14		 81/35/65	3545/886
15		 >99/34/66	4333/1083

## Nitro compounds

16		 72	3152/788
17		 95	4158/1040
18		 74	3239/820
19		 >99	4333/1083
20		 79/100	3457/864
21		 69/100	3020/755

22			2538/635
		58/100	
23			2932/733
		67/100	
24			2188/547
		50/91	

## Hydrodehalogenation

25			1838/460
		42/25/75	
26			4333/1083
		>99/100	
27			2188/547
		50/9/91	
28			4333/1083
		>99/100	
29			3851/963
		88/18/82	

Reaction conditions: Substrate (9.87 mmol), conc. of Pd (0.023 mol%), substrate/catalyst ratio (4377/1), H<sub>2</sub>O (50 mL), temperature (50 °C), H<sub>2</sub> pressure (8 bar), time (4 h).

### Comparison with reported catalyst

Catalytic activity of the present catalyst is also compared with reported catalysts for C-C coupling reactions (Table 11 & 12) in terms of iodobenzene and hydrogenation reaction (Table 13) in terms of cyclohexene as one of the substrates.

It is seen for SM coupling (Table 11), that present catalyst is superior in terms of mol% of Pd, TON as well as TOF compared to all reported catalytic systems.

**Table 11** Comparison of catalytic activity for SM coupling with reported catalyst in organic-water solvent mixture with respect to iodobenzene

Catalyst	Pd (mol %)	Solvent	Temp. (°C)/Time (h)	% Conversion/TON /TOF (h <sup>-1</sup> )
Pd-ScBTC NMOFs [32]	0.5	C <sub>2</sub> H <sub>5</sub> OH: H <sub>2</sub> O (1:1 mL)	40/0.5	99/194/388
Pd/C [33]	0.37	C <sub>2</sub> H <sub>5</sub> OH: H <sub>2</sub> O (1:1 mL)	40/0.5	99/268/535
Oximepalladacycle catalyst [34]	0.3	C <sub>2</sub> H <sub>5</sub> OH: H <sub>2</sub> O (1:1 mL)	RT/0.3	95/317/1057
Fe <sub>3</sub> O <sub>4</sub> /Ethyl-CN/Pd [35]	0.2	C <sub>2</sub> H <sub>5</sub> OH: H <sub>2</sub> O (1:1 mL)	RT/0.2	98/49/245
G-BI-Pd [36]	0.45	C <sub>2</sub> H <sub>5</sub> OH: H <sub>2</sub> O (1:1 mL)	80/0.084	98/219/2613
<b>PdTPA/SiO<sub>2</sub> (Present catalyst)</b>	<b>0.0192</b>	<b>C<sub>2</sub>H<sub>5</sub>OH: H<sub>2</sub>O (3:7 mL)</b>	<b>90/0.5</b>	<b>94/4902/9804</b>

**Table 12** Comparison of catalytic activity for Heck reaction with reported catalysts with respect to iodobenzene

Catalyst	Pd (mol %)	Solvent	Temp. (°C)/Time (h)	% Conversion/TON/ TOF (h <sup>-1</sup> )
PdTSPc@KP-GO [37]	0.792	H <sub>2</sub> O (10 mL)	reflux/9	89/111/12
Pd/CNCs [38]	1.412	DMF (10 mL)	40/5	93/65/13
NO <sub>2</sub> -NHC- Pd@Fe <sub>3</sub> O <sub>4</sub> [39]	1.0	CH <sub>3</sub> CN (5 mL)	80/5	96/96/19
5% Pd/CM [40]	0.2	DMA	80/24	61/3050/127
PFG-Pd [41]	1.7	DMF (3 mL)	120/6	95/56/9
<b>PdTPA/SiO<sub>2</sub> (Present catalyst)</b>	<b>0.115</b>	<b>DMF: H<sub>2</sub>O (3:2 mL)</b>	<b>100/6</b>	<b>94/817/136</b>

In case of Heck coupling (Table 12) also, present catalyst is found superior in terms of the used solvent medium, mol% of Pd, % conversion as well as high TON/TOF.



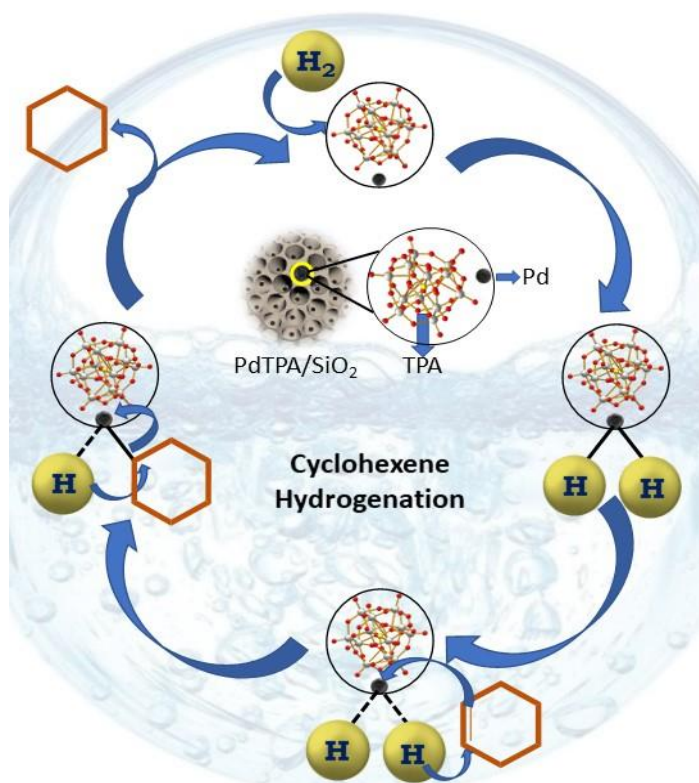
**Table 13** Comparison with the reported catalyst with respect to cyclohexene hydrogenation

Catalyst	Pd (mol%)	Solvent	Temp. (°C)	Pressure (bar)	% Conv./TON/TOF
SH-IL-1.0wt%Pd [42]	0.02	Auto- clave	60	20	99/5000/5000
Pd/MSS@ZIF-8 [43]	0.1738	Ethyl acetate	35	1	5.6/560/93
Pd@CN [44]	2.208	Formic acid	90	(Proton transfer)	96/44/3.67
Pd/SiO <sub>2</sub> [28]	0.091	CO <sub>2</sub> (60 bar)	25	10	96/1097/6582
<b>PdTPA/SiO<sub>2</sub> (Present catalyst)</b>	<b>0.023</b>	<b>Water</b>	<b>50</b>	<b>8</b>	<b>97/4245/1061</b>

In case of hydrogenation, the true competence of the presented catalyst is also compared with reported systems (Table 13). Liu et al. [42] reported high conversion at a lower temperature, with the utilization of very high H<sub>2</sub> pressure (20 bar) for the reaction compared to present work. Zhang et al. [43] reported the reaction at 35 °C with very poor conversion, moreover a mole % of catalyst was too high. Leng et al. [44] achieved high conversion using formic acid as an *in-situ* proton transferring agent with a very high concentration of the Pd compared to the present catalytic system along with very low TON. Panpranot et al. [28] achieved excellent conversion using supercritical CO<sub>2</sub> as a solvent at 60 bar pressure (extremely high condition). Enumerated data of table 13 indicates that the present catalytic system is best one of all reported one in terms of activity under mild reaction conditions.

## Mechanistic investigation of cyclohexene hydrogenation

The mystery of the mechanism was exposed by control experiments and deuterated water as solvent. (i) *Control experiments*: In order to investigate the active species, the reaction was carried out with  $\text{SiO}_2$ , TPA,  $\text{PdCl}_2$ , PdTPA and PdTPA/ $\text{SiO}_2$  under identical conditions. Obtained results (Table 6) clearly shows that Pd is the only active centres responsible for the reaction. (ii) *Under  $\text{N}_2$  pressure*: To confirm the necessity of the  $\text{H}_2$ , the reaction was examined by carrying out the reaction under  $\text{N}_2$  pressure instead of  $\text{H}_2$ . In result, no conversion was found, which clearly indicates the essentiality of  $\text{H}_2$  for the reaction. (iii)  *$\text{D}_2\text{O}$  as solvent*: In order to understand the role of water, as proton transferring agent or solvent only, reaction was carried using  $\text{D}_2\text{O}$  as solvent instead of  $\text{H}_2\text{O}$ . Absence of deuterated product (confirmed by  $^1\text{H}$  NMR) in isolated product (i.e. cyclohexane) revealed the hydrogen transfer directly from  $\text{H}_2$  gas, not from water. Based on this data, scheme 3 shows the proposed mechanism.



**Scheme 3** Proposed reaction mechanism.

### Comparison study of PdTPA/ZrO<sub>2</sub> and PdTPA/SiO<sub>2</sub>

In order to compare the activity of the catalysts, both coupling and hydrogenation reactions were carried out under identical experimental conditions. Obtained results (Table 14) are compared in terms of % conversion, TON/TOF.

**Table 14** Effect of support on conversion % conversion, TON/TOF

Catalyst	Total acidity (mequi./g)	SM coupling		Heck coupling		Hydrogenation		Surface area (m <sup>2</sup> /g)
		% Conv.	TON/ TOF	% Conv.	TON/ TOF	% Conv.	TON/ TOF	
PdTPA/ZrO <sub>2</sub>	4.7	96	5006/ 10012	96	834/ 139	60	2627/ 657	202
PdTPA/SiO <sub>2</sub>	5.1	94	4902/ 9804	94	817/ 136	97	4245/ 1061	322

Reaction conditions: *SM coupling*- iodobenzene (1.96 mmol), phenylboronic acid (2.94 mmol), K<sub>2</sub>CO<sub>3</sub> (3.92 mmol), conc. of Pd (0.0192 mol%), substrate/catalyst ratio (5215/1), C<sub>2</sub>H<sub>5</sub>OH: H<sub>2</sub>O (3:7 mL), time (30 min), temperature (90 °C); *Heck coupling*- iodobenzene (1.96 mmol), phenylboronic acid (2.94 mmol), K<sub>2</sub>CO<sub>3</sub> (3.92 mmol), conc. of Pd (0.115 mol%), substrate/catalyst ratio (869/1), DMF: H<sub>2</sub>O (3:2 mL), time (6 h), temperature (100 °C); *Hydrogenation*- Cyclohexene (9.87 mmol), conc. of Pd (0.023 mol%), substrate/catalyst ratio (4377/1), H<sub>2</sub>O (50 mL), time (4 h), temperature (50 °C), H<sub>2</sub> pressure (8 bar).

In case of C-C coupling, the results show that PdTPA/ZrO<sub>2</sub> is more active compared to PdTPA/SiO<sub>2</sub>. This can be explained on the basis of total acidic sites. The high activity of PdTPA/ZrO<sub>2</sub> is attributed to its lower acidity compared to PdTPA/SiO<sub>2</sub>. As base K<sub>2</sub>CO<sub>3</sub> was used in the reaction, which is necessary for the transmetallation step for the formation of product, gets neutralized with acidity of the catalyst and lowers the rate of the reaction. As a result, PdTPA/ZrO<sub>2</sub> is more active than PdTPA/SiO<sub>2</sub>.

In case of hydrogenation, obtained results (Table 14) show that PdTPA/SiO<sub>2</sub> is more active than PdTPA/ZrO<sub>2</sub>. This can be explained on the basis of surface area. The surface area of PdTPA/SiO<sub>2</sub> (322 m<sup>2</sup>/g) is higher compared to

PdTPA/ZrO<sub>2</sub> (202 m<sup>2</sup>/g). It is well known that high surface area makes successful collision of substrates more feasible and accelerates the hydrogenation rate, as a result PdTPA/SiO<sub>2</sub> is more active than the rest one. Activity order of the catalysts is:

**C-C Coupling: PdTPA/ZrO<sub>2</sub> > PdTPA/SiO<sub>2</sub>**

**Hydrogenation: PdTPA/SiO<sub>2</sub> >> PdTPA/ZrO<sub>2</sub>**

## Conclusion

- Synthesis of encapsulated stabilized PdNCLs by 12-tungstophosphoric acid (PdTPA/SiO<sub>2</sub>) was carried out successfully by impregnation and post reduction method
- FT-IR, <sup>31</sup>P MAS NMR and XRD confirm the retention of Keggin structure, XPS confirms the oxidation states of Pd(0) and W(VI), whereas TEM, HRTEM and STEM confirm the encapsulation of PdNCLs into the support
- The supported catalyst depicts outstanding activity for C-C coupling (SM and Heck) and hydrogenation
- Leaching and heterogeneity test confirms that present catalyst is truly heterogeneous in nature
- The catalyst can be recycled, regenerated and reused up to five cycles (and can be used for more) without significant loss in catalytic activity
- EDX, BET, FT-IR, XPS and TEM of regenerated catalyst show no structural changes indicating the stability of the catalyst
- Substrate study shows that catalyst is highly viable towards different variety of the substrates
- A detailed reaction mechanism for cyclohexene hydrogenation in water is discussed
- PdTPA/ZrO<sub>2</sub> presents superior catalytic activity towards C-C coupling whereas PdTPA/SiO<sub>2</sub> shows towards hydrogenation compared to each other indicating that acidity of the catalyst plays an important role in C-C coupling whereas, surface area in hydrogenation reaction

---

**References**

- [1] J. M. Thomas, R. Raja and D. W. Lewis, *Angew. Chem. Int. Ed.*, 44, 6456-6482, (2005).
- [2] J. C. Vartuli and T. F. Degnan, in: *Studies in Surface Science and Catalysis*, Vol. 168, eds. J. Čejka, H. van Bekkum, A. Corma and F. Schüth, Elsevier, 2007).
- [3] K.-i. Otake, J. Ye, M. Mandal, T. Islamoglu, C. T. Buru, J. T. Hupp, M. Delferro, D. G. Truhlar, C. J. Cramer and O. K. Farha, *ACS Catal.*, 9, 5383-5390, (2019).
- [4] J.-H. Smått, C. Weidenthaler, J. B. Rosenholm and M. Lindén, *Chem. Mater.*, 18, 1443-1450, (2006).
- [5] H. Zhang, G. Hardy, Y. Khimyak, M. Rosseinsky and A. Cooper, *Chem. Mater.*, 16, 4245-4256, (2004).
- [6] R. Raja and J. M. Thomas, in: *Model Systems in Catalysis*, Springer, 2010).
- [7] G. D. Parfitt, in: *Progress in Surface and Membrane Science*, Vol. 11, eds. D.A. Cadenhead and J.F. Danielli, Elsevier, 1976).
- [8] J. Westall and H. Hohl, *Adv. Colloid Interface Sci.*, 12, 265-294, (1980).
- [9] T. W. Healy and D. W. Fuerstenau, *J. Colloid Sci.*, 20, 376-386, (1965).
- [10] H. P. Boehm, *Discuss. Faraday Soc.*, 52, 264-275, (1971).
- [11] S. Muhammad, S. T. Hussain, M. Waseem, A. Naeem, J. Hussain and M. Jan, *Iranian J. Sci. Technol., Trans. A: Sci.*, 36, 481-486, (2012).
- [12] J.-P. Cloarec, C. Chevalier, J. Genest, J. Beauvais, H. Chamas, Y. Chevolot, T. Baron and A. Souifi, *Nanotechnol.*, 27, 295602, (2016).
- [13] N. Mizuno, J.-S. Min and A. Taguchi, *Chem. Mater.*, 16, 2819-2825, (2004).
- [14] I. Kozhevnikov, K. Kloetstra, A. Sinnema, H. Zandbergen and H. v. van Bekkum, *J. Mol. Catal. A: Chem.*, 114, 287-298, (1996).
- [15] T. Okuhara, N. Mizuno and M. Misono, *Appl. Catal., A*, 222, 63-77, (2001).
- [16] C. Bianchini, D. G. Burnaby, J. Evans, P. Frediani, A. Meli, W. Oberhauser, R. Psaro, L. Sordelli and F. Vizza, *J. Am. Chem. Soc.*, 121, 5961-5971, (1999).

- 
- [17] A. Patel and S. Singh, *Micropor. Mesopor. Mater.*, 195, 240-249, (2014).
- [18] A. Popa, V. Sasca, E. E. Kiss, R. Marinkovic-Neducin, M. T. Bokorov and I. Holclajtner-Antunović, *Mater. Chem. Phys.*, 119, 465-470, (2010).
- [19] J. Martínez, S. Palomares-Sánchez, G. Ortega-Zarzosa, F. Ruiz and Y. Chumakov, *Mater. Lett.*, 60, 3526-3529, (2006).
- [20] A. V. Matveev, V. V. Kaichev, A. A. Saraev, V. V. Gorodetskii, A. Knop-Gericke, V. I. Bukhtiyarov and B. E. Nieuwenhuys, *Catal. Today*, 244, 29-35, (2015).
- [21] Y. Leng, C. Zhang, B. Liu, M. Liu, P. Jiang and S. Dai, *ChemSusChem*, 11, 3396-3401, (2018).
- [22] R. Villanneau, A. Roucoux, P. Beaunier, D. Brouri and A. Proust, *RSC Adv.*, 4, 26491-26498, (2014).
- [23] L. D'Souza, M. Noeske, R. M. Richards and U. Kortz, *Appl. Catal., A*, 453, 262-271, (2013).
- [24] L. D'Souza, M. Noeske, R. M. Richards and U. Kortz, *J. Colloid Interface Sci.*, 394, 157-165, (2013).
- [25] S. Rana and K. M. Parida, *Catal. Sci. Technol.*, 2, 979-986, (2012).
- [26] R. A. Sheldon, M. Wallau, I. W. C. E. Arends and U. Schuchardt, *Acc. Chem. Res.*, 31, 485-493, (1998).
- [27] S. Singh and A. Patel, *J. Cleaner Prod.*, 72, 46-56, (2014).
- [28] J. Panpranot, K. Phandinthong, P. Praserttham, M. Hasegawa, S. I. Fujita and M. Arai, *J. Mol. Catal. A: Chem.*, 253, 20-24, (2006).
- [29] Y. Wang, A. V. Biradar and T. Asefa, *ChemSusChem*, 5, 132-139, (2012).
- [30] C. Xia, J. Xu, W. Wu and X. Liang, *Catal. Commun.*, 5, 383-386, (2004).
- [31] F. Urbano and J. Marinas, *J. Mol. Catal. A: Chem.*, 173, 329-345, (2001).
- [32] L. Zhang, Z. Su, F. Jiang, Y. Zhou, W. Xu and M. Hong, *Tetrahedron*, 69, 9237-9244, (2013).
- [33] Z. Shi and X.-F. Bai, *Open Mater. Sci. J.*, 9, 173-177, (2015).
- [34] M. Gholinejad, M. Razeghi and C. Najera, *RSC Adv.*, 5, 49568-49576, (2015).
-

- [35] B. Abbas Khakiani, K. Pourshamsian and H. Veisi, *Appl. Organomet. Chem.*, 29, 259-265, (2015).
- [36] M. Sarvestani and R. Azadi, *Appl. Organomet. Chem.*, 31, e3667, (2016).
- [37] Z. Hezarkhani and A. Shaabani, *RSC Adv.*, 6, 98956-98967, (2016).
- [38] X.-W. Guo, C.-H. Hao, C.-Y. Wang, S. Sarina, X.-N. Guo and X.-Y. Guo, *Catal. Sci. Technol.*, 6, 7738-7743, (2016).
- [39] V. Kandathil, B. D. Fahlman, B. S. Sasidhar, S. A. Patil and S. A. Patil, *New J. Chem.*, 41, 9531-9545, (2017).
- [40] Y. Monguchi, F. Wakayama, S. Ueda, R. Ito, H. Takada, H. Inoue, A. Nakamura, Y. Sawama and H. Sajiki, *RSC Adv.*, 7, 1833-1840, (2017).
- [41] R. Fareghi-Alamdari, M. G. Haqiqi and N. Zekri, *New J. Chem.*, 40, 1287-1296, (2016).
- [42] R. Tao, S. Miao, Z. Liu, Y. Xie, B. Han, G. An and K. Ding, *Green. Chem.*, 11, 96-101, (2009).
- [43] T. Zhang, B. Li, X. Zhang, J. Qiu, W. Han and K. L. Yeung, *Micropor. Mesopor. Mater.*, 197, 324-330, (2014).
- [44] C. Zhang, Y. Leng, P. Jiang, J. Li and S. Du, *Chem. Select*, 2, 5469-5474, (2017).